E.C.APAK METU 2006

A STUDY ON HEAT TRANSFER INSIDE THE WELLBORE DURING DRILLING OPERATIONS

ESAT CAN APAK

DECEMBER 2006

A STUDY ON HEAT TRANSFER INSIDE THE WELLBORE DURING DRILLING OPERATIONS

A THESIS SUBMITTED TO
THE GRADUATE SCHOOL OF NATURAL AND APPLIED SCIENCES
OF
MIDDLE EAST TECHNICAL UNIVERSITY

BY

ESAT CAN APAK

IN PARTIAL FULFILLMENT OF THE REQUIREMENTS
FOR
THE DEGREE OF MASTER OF SCIENCE
IN
PETROLEUM AND NATURAL GAS ENGINEERING

DECEMBER 2006

Approval of the Graduate School of Natural and Applied Sciences of Middle East Technical University.

Prof. Dr. Canan Özgen
Director

I certify that this thesis satisfies all the requirements as a thesis for the degree of Master of Science.

Prof. Dr. Mahmut Parlaktuna
Head of Department

This is to certify that we have read this thesis and that in our opinion it is fully adequate, in scope and quality, as a thesis for the degree of Master of Science.

Assist. Prof. Dr. Evren Özbayoğlu
Supervisor

Examining Committee Members

Prof. Dr. Mahmut Parlaktuna	(METU,PETE)	
Assist. Prof. Dr. Evren Özbayoğlu	(METU,PETE)	
Prof. Dr. Mustafa V. Kök	(METU,PETE)	
Prof. Dr. Birol M.R. Demiral	(METU,PETE)	
Prof. Dr. Nurkan Karahanoğlu	(METU,GEOE)	

I hereby declare that all information in this document has been obtained and presented in accordance with academic rules and ethical conduct. I also declare that, as required by these rules and conduct, I have fully cited and referenced all material and results that are not original to this work.

Name, Last name : Esat Can Apak

Signature :

ABSTRACT

A STUDY ON HEAT TRANSFER INSIDE THE WELLBORE
DURING DRILLING OPERATIONS

Apak, Esat Can
M. Sc., Department of Petroleum and Natural Gas Engineering
Supervisor: Assist.Prof.Dr. Evren Özbayoğlu

December 2006, 85 pages

Analysis of the drilling fluid temperature in a circulating well is the main objective of this study. Initially, an analytical temperature distribution model, which utilizes basic energy conservation principle, is presented for this purpose. A computer program is written in order to easily implement this model to different cases. Variables that have significant effect on temperature profile are observed. Since the verification of the analytical model is not probable for many cases, a computer program (ANSYS) that uses finite element method is employed to simulate different well conditions. Three different wells were modeled by using rectangular FLOTRAN CFD element that has four nodes. Maximum drilling fluid temperature data corresponding to significant variables is collected

from these models. This data is then used to develop an empirical correlation in order to determine maximum drilling fluid temperature. The proposed empirical correlation can estimate the temperature distribution within the wellbore with an average error of less than 16%, and maximum drilling fluid temperature with an average error of less than 7 %.

Keywords: Temperature Distribution, Maximum Drilling Fluid Temperature, Drilling Fluid, ANSYS Thermal Analysis

ÖZ

SONDAJ ESNASINDA KUYU İÇERİSİNDEKİ ISI AKTARIMI
İLE İLGİLİ BİR ÇALIŞMA

Apak, Esat Can
Yüksek Lisans, Petrol ve Doğal Gaz Mühendisliği Bölümü
Tez Yöneticisi: Yar.Doç.Dr. Evren Özbayoğlu

Aralık 2006, 85 Sayfa

Bu çalışmanın ana hedefi, sirkülasyon halindeki bir kuyudaki sondaj sıvısının sıcaklık analizidir. Bu bağlamda ilk olarak, temel enerji korunumu yasasına dayanan bir analitik sıcaklık dağılım modeli sunulmuştur. Bu modelin farklı durumlarda rahatça uygulanabilmesi için bir program yazılmıştır. Sıcaklık profiline etkisi dikkate değer olan değişkenler gözlenmiştir. Analitik modelin birden fazla durumda sınanması olanaklı olmadığı için, farklı kuyu koşullarını taklit etmek amacıyla sınırlı eleman yöntemi ile çözüm yapan bir bilgisayar programı (ANSYS) kullanılmıştır. Dört nodu olan dörtgen FLOTRAN CFD elemanı kullanılarak üç farklı kuyu modellenmiştir. Dikkate değer değişkenlere karşılık gelen azami sondaj sıvısı sıcaklıklığı verileri bu modeller kullanılarak

toplanmıştır. Sonra bu veriler, en yüksek sondaj sıvısı sıcaklığını belirlemek amaçlı ampirik bir bağıntı kurmak için kullanılmıştır. Elde edilen ampirik denklem, kuyu içerisindeki sıcaklık dağılımını ortalama % 16'dan, en yüksek sıcaklık değerlerini ortalama % 7'den küçük bir hata payı ile tahmin edebilmektedir.

Anahtar Kelimeler: Sıcaklık Dağılımı, En Yüksek Sondaj Sıvısı Sıcaklığı, Sondaj Sıvısı, ANSYS, ANSYS Termal Analiz

ACNKOWLEDGEMENTS

I would like to thank my advisor Assist.Prof.Dr. M. Evren Özbayoğlu for his valuable support, guidance and encouragement during this study. My thesis committee members Prof. Dr. Mahmut Parlaktuna, Prof Dr. M. Evren Özbayoğlu, Prof. Dr. Mustafa V. Kök, Prof. Dr. Birol M.R. Demiral and Prof. Dr. Nurkan Karahanoğlu are very appreciated for their comments and suggestions.

TABLE OF CONTENTS

PLAGIARISM iii
ABSTRACT iv
ÖZ vi
ACNKOWLEDGEMENTS viii
TABLE OF CONTENTS ix
LIST OF FIGURES xi
LIST OF TABLES xiii
NOMENCLATURE 1
CHAPTER
1. INTRODUCTION 3
2. LITERATURE REVIEW 6
2.1. Change of Drilling fluid Characteristics with Temperature 6
2.2. Heat Exchange Analyses 8
3. STATEMENT OF THE PROBLEM 11
4. SCOPE 13
5. THEORY 14
5.1. Assumptions 14
5.2. Derivations 16
5.3. Application of the Equations to Casing and Cement Layers 26
6. COMPUTER WORK 28
7. RESULTS AND DISCUSSION 33
7.1. Results from Analytical Solution 33
7.2. Results from Computer Work 42
7.2.1. Simulation Data 42

7.2.2. Correlation Results 50
7.3. Comparison 54
8. CONCLUSION 55
REFERENCES 57
APPENDICES
A. HOLMES AND SWIFT'S STEADY STATE MODEL 59
B. SAMPLE CALCULATION FOR OPEN HOLE WELL 62
C. SAMPLE CALCULATION FOR A WELL WITH THREE CASING STRINGS 66
D. A SAMPLE SIMULATION RUN 71

LIST OF FIGURES

Figure 1. Diagram of the wellbore that has a length of dx. 16
Figure 2. Different casing and cement layers in a wellbore 27
Figure 3. Element view of the 1640 ft model. 30
Figure 4. Wellbore geometry at the bottom. 30
Figure 5. Change of temperature with respect to depth in the 1640 ft model. 31
Figure 6. Temperature profile comparison with Holmes and Swift [9] Model 34
Figure 7. Temperature profile comparison with Holmes and Swift [9] Model 35
Figure 8. Change of temperature profile with different flow rates 36
Figure 9. Change of maximum temperature with pump rate 37
Figure 10. Change of temperature profile with different circulation time 38
Figure 11. Change of maximum temperature with circulation time 39
Figure 12. Temperature distribution in a well with casing strings. 40
Figure 13. Temperature distribution in a 5000 ft well. 41
Figure 14. Change of temperature profile with different flow rates and time values at 1640 ft well. 43
Figure 15. Change of temperature distribution with formation conductivity. 44
Figure 16. Change of temperature distribution with formation specific heat. 45
Figure 17. Change of temperature distribution with inlet fluid. 46
Figure 18. Change of temperature distribution with surface earth temperature (^{o}F). 47
Figure 19. Change of temperature profile with different flow rates and time velues at 3280 ft well. 48
Figure 20. Change of temperature profile with different flow rates and time velues at 4920 ft well. 49

Figure 21. Correlation results with simulation data. 50
Figure 22. Accuracy of temperature approximation in the annulus. 51
Figure 23. Accuracy of temperature approximation in the drill pipe. 52
Figure 24. Accuracy of maximum temperature estimation. 53
Figure 25. Simulation and analytically calculated data comparison. 54
Figure 26. Diagram of the wellbore that has a length of dx (Used in Holmes & Swift [10] Model). 59
Figure 27. Casing strings used in sample calculation 66
Figure 28. Sample simulation run. 71

LIST OF TABLES

Table 1. Well and mud data from Holmes and Swift..... 62

NOMENCLATURE

α	heat diffusivity of formation, sq ft/hr
A_p	cross-sectional area of inside of the drillpipe, sq-ft
A_a	cross-sectional area of inside of the annulus, sq-ft
c_f	specific heat of formation, BTU/(lb-^{o}F)
c_p	specific heat of drilling fluid, BTU/(lb-^{o}F)
G	geothermal gradient, ^{o}F/ft
h_a	coefficient of heat transfer of fluid in annulus, BTU/day-sq ft-^{o}F
h_p	coefficient of heat transfer of fluid in drillpipe, BTU/day-sq ft-^{o}F
H	well depth, ft
k_c	thermal conductivity of casing, BTU/(ft-^{o}F-hour)
k_e	thermal conductivity of cement, BTU/(ft-^{o}F-hour)
k_p	thermal conductivity of drillpipe, BTU/(ft-^{o}F-hour)
k_f	thermal conductivity of formation, BTU/(ft-^{o}F-hour)
k	thermal conductivity of drilling fluid, BTU/(ft-^{o}F-hour)
m	mass flow rate, lb/hr
N_{Pr}	Prandtl number
N_{REp}	Reynold's number for drillpipe
N_{REa}	Reynold's number for drillpipe
q	Volumetric flow rate, Bbl/hr
$\dot{Q}_{ap}$	conductive heat flow across drillpipe, BTU/hr
$\dot{Q}_{af}$	conductive heat flux from formation, BTU/hr
$\dot{Q}_a$	convective heat flow in the annulus, BTU/hr

$\dot{Q}_p$	convective heat flow in the drillpipe, BTU/hr
$\dot{Q}$	convective heat flux from wellbore, BTU/hr
ρ_f	density of formation, lb/gal
ρ	density of drilling fluid, lb/gal
r_{pi}	drillpipe inner radius, ft
r_{po}	drillpipe outer radius, ft
r_{ci}	casing inner radius, ft
r_{co}	casing outer radius, ft
r_{wb}	formation sand face radius, ft
t	circulation time, hr
T_D	dimensionless temperature
T_{pi}	drillpipe inlet fluid temperature, ^oF
T_s	surface earth temperature, ^oF
T_{wb}	temperature at wellbore-formation interface, ^oF
T_a	fluid temperature in the annulus, ^oF
T_p	fluid temperature in the drillpipe, ^oF
T_f	temperature of the formation, ^oF
T_{max}	maximum fluid temperature in a well, ^oF
t_D	dimensionless time
U_p	overall heat transfer coefficient from annulus to drillpipe, BTU/day-sq ft-^oF
U_a	overall heat transfer coefficient from formation to annulus, BTU/day-sq ft-^oF

CHAPTER 1

INTRODUCTION

Drilling fluid, so called "mud", is one of the most essential components needed during drilling operations. Due to its nature as the buffer between the drilled rock and drilling equipment, drilling fluid must be prepared anticipating every possible change in the environment. It must be carefully engineered to accommodate different functions such as lubrication, cleaning the bit surface, transporting the cuttings and providing hydrostatic pressure to compensate for the formation pressure. While some of these functions may be accomplished by a static fluid column, others would only be achieved in a dynamic environment. In conventional drilling, drilling fluid is sucked from the drilling fluid tank using a pump, goes through the surface lines and drillstring, flows through the bit and flows up through the annulus to the surface and goes back to the drilling fluid tank after some treatment; thus forms a continuous circulation. Apart from its other functions and assuming the circulation is continuous as in a normal case, drilling fluid cools down the formation around the hole. As the depth of the well increases, so does the temperature due to the geothermal gradient of the earth. This process may heat the fluid to dangerous temperatures and cause a problem.

Conventional drilling fluid is basically divided into two categories as, water based drilling fluids and oil based drilling fluids. Water based drilling fluid, which is more frequently used and will be the main focus of this study, is typically composed of water, clay minerals and other additives. Some of these

chemicals react with water to increase viscosity and induce gel forming capability. Additives are used to limit these reactions in order to control the function of the drilling fluid inside desired limits. According to several authors [1-5], increasing temperature causes two primary problems: flocculation and dispersion.

Gel strength of the fluid dramatically increases and wool like structures, namely floccules forms. Increasing the shear rate of the fluid, in other words increasing the pumping rate and rotary speed could undo some of the damage done by flocculation. However, as the exposure time to the high temperature increases, so does the number of individual platelets in suspension due to dispersion of clay minerals and this would permanently increase the viscosity [4].

Contamination of the drilling fluid from the formation, which is a normal occurrence in a drilling operation, may multiply these reactions. Solubility of many minerals in water increases with the rising temperature. Ionization of these minerals in water may change the ion concentrations. Since clay particles have charged surfaces, any shift in the ion concentrations makes the prediction of downhole drilling fluid behavior very difficult [7].

These effects would have detrimental results in the field such as drilling fluid becoming nearly solid, observation of pressure spikes or losses [8] and log tools that would not get to the bottom of the well. So, physical and chemical properties of a fluid flowing in a well are affected by temperature, therefore determination of temperature profile of fluids in circulating well is very important. Temperatures in both drillpipe and annulus must be known in order to predict and avoid possible problems. It may also aid calculating the time that would take the drilling fluid to begin showing degradation, if the circulation comes to a halt. A good estimation of maximum drilling fluid temperature would help selecting and preparing the drilling fluid.

To develop a model, heat transfer inside the wellbore must be carefully analyzed. The problem could be separated into two parts: 1) Fluid, that is flowing down in the drillpipe is heated by the annular fluid, and 2) Annular fluid, that is flowing up in the annulus gets heat energy from formation directly or through the layers of cement and casing strings and transfers heat to the fluid in drillpipe. Heat transfer is influenced by many parameters, but some of these are neglected due to their very small impact on the final solution like heat generation due to friction and heat from cuttings, in order to keep the model simple enough be easily used in the field. The main effect is done by pumping rate, which if increased reduces the temperature and circulation time, which as increases formation cools down and reduces the drilling fluid temperature.

Several analytical models exist, but they are neither easily applicable in field, nor they are tested and compared to real field data. Since measuring temperature in all points of a well is impossible, testing the models is difficult. This study focuses on creating the downhole conditions in a virtual environment, comparing the data obtained with an analytic model and ultimately proposing an empirical correlation that will be accurate and easy to use.

CHAPTER 2

LITERATURE REVIEW

In 1950's, number of geothermal or deep oil wells drilled boosted dramatically, due to depletion of shallow reservoirs and progression of geothermal energy as an alternative to fossil fuels. The need to explain drilling fluid related problems and counter amend them was only a natural engineer instinct. Starting with 1955, subject of effects of high temperature on drilling fluids became popular, and a few years later first heat transfer studies began to emerge.

2.1. Change of Drilling fluid Characteristics with Temperature

Sirini-Vasan et al. [1] were the first to analyze the effect of temperature on flow properties of water based drilling fluids in 1957. With limited equipment, which consisted of a laboratory model Fann V-G meter with an aluminum water jacket around the drilling fluid cup, they made some high temperature experiments on different types of drilling fluids. The results showed that plastic viscosity decreased with increasing temperature. They tried to basically correlate this data to approximate plastic viscosity at downhole conditions. They also collected gel strength data but did not attempt to use it.

Five years later Hiller [2] published a more detailed study. He designed and used a rotational viscometer that is capable of reaching very high temperature and

pressure (350 ^{o}F and 10000 psi respectively). Conclusions reached were that flow properties of drilling fluids differed considerably under bottom-hole conditions from surface conditions and these differences were not generally predictable. He showed that even chemically similar drilling fluids could have very different behaviors. Although the data seemed unparallel, he proposed a relationship between fluids with similar ionization pattern, but he made no effort to make a correlation.

As the wells got deeper and hotter, previous studies became insufficient. Weintritt et al. [3] have devised an apparatus by modifying a cement consistometer to measure relative viscosity of drilling fluids at temperatures approaching 500 ^{o}F. The results of this work showed that when the clays are heated over 250 ^{o}F, chemical and colloid equilibrium would change and a change in active solid content of the drilling fluid might have detrimental effects on the drilling fluid properties.

Annis [4] conducted experiments with a modified conventional and a newly designed HP-HT concentric-cylinder rotational viscometers of the Fann type, to analyze the rheological and gel property changes due to elevated temperatures in 1967. Factors that affect viscosity of a drilling fluid were primarily defined as flocculation and dispersion. He pointed out that high temperature causes flocculation of bentonitic clays, resulting in high yield points, high viscosities at low shear rates and high gel strength, and dispersion of bentonitic clays resulting in a permanent thickening of the drilling fluid.

Insufficiency of deflocculants available was shown by Chesser et al. [5] in 1980. Additives were listed with their thermal degradation limits and a new copolymer was introduced that would extend the temperature range of the water-base drilling fluid safely to 500 ^{o}F.

Nowadays, environmental and economic concerns drive research. A more recent study by Amanullah [6] was on a new degradation inhibitor that is cheap and environment friendly.

2.2. Heat Exchange Analyses

As work on understanding and preventing drilling fluid degradation with elevated temperatures progressed, so did studies that analyzes heat exchange in a wellbore in order to understand the temperature distribution. Different analytical and numerical models [9-11] have emerged since early 60's, some of which has roots to Ramey's model [9] presented in 1962. He proposed an approximation for heat-transmission problem involved in injection of hot or cold fluids. The temperature of fluid was expressed as a function of depth and time. The assumptions were that the heat transfer in the wellbore was steady-state, whereas heat transfer to or from the formation was unsteady radial conduction. Although his work is old and lacks the necessary modifications needed to predict temperature distribution at early times, the results obtained from his model are very accurate. A recent paper by Hagoort [20] presented some modifications and corrections to Ramey's model.

First analytical solution to temperature profile during drilling was developed in 1969 by Holmes et al. [10]. This was a basic work that assumed steady-state linear heat transfer from the formation to the drilling fluid. While the model gave good approximation for the time being, the temperature drop after long periods of circulation was not left unexplained.

Raymond [11] claimed that the bottomhole fluid temperature continually changed with time and never attained a steady-state condition. With a similar approach, he defined temperature profile in the drillpipe as a function of downward convection, conduction from annulus and time and temperature profile in the annulus as a function of conduction to drillpipe, upwards convection, conduction

from formation and time. The resulting model was complex and solved numerically. It had little practical field use. Raymond devised ΔT vs. Q charts by simulating circulation in over 70 wells in order to be used to easily calculate bottom-hole fluid temperature by only using annulus outlet temperature, drilling fluid density, and depth after 5 to 6 hours of circulation. However, the charts were only prepared for a fixed geothermal gradient, drillpipe and hole size.

Keller et al. [12] developed a numerically solved model describing two-dimensional transient heat transfer in and around a wellbore in 1973. The effects of the viscous flow energy, rotational energy and drill bit energy were included in the model. They compared their work with previous steady-state studies and observed that results were similar. The equations devised were adaptable to different casing and cement layers. Solution was reached by employing finite difference equations. Overall heat coefficient that approximates the resistance to heat flow through different layers of fluid and solid was not used.

Need for a simpler though effective solution led Thompson et al. [14] to develop a computer model that is fast in execution. They have used a one-dimensional transient model and employed the method of characteristics to solve it. A computer program was developed for field practices. Some validation of the program with field data has been provided.

In a more recent study, Kabir et al. [17] presented a simpler analytical model for predicting temperature profiles during normal and reverse circulation. Similar to Ramey's model [8], they assumed steady-state heat transfer in wellbore and transient heat-transfer in the formation. They employed dimensionless temperature function to approximate heat flow from the formation. Same well and drilling fluid data from Holmes et al. [9] was used to verify the solution.

Kabir et al. [18] progressed their work with another paper published in the same year. They claimed that temperature of the fluid entering wellbore from the

holding tank would not stay constant because of the heat brought back by the annular fluid. A slight modification was made to compensate for holding tank temperature change.

CHAPTER 3

STATEMENT OF THE PROBLEM

Most of the shallow reservoirs have been explored and developed, but search for oil and gas continues in deeper formations. As wells get deeper, temperature slowly rises and it gets to a point which drilling fluid degradation occurs. There are cases like geothermal energy and mineral extraction from steam or hot water that requires hot wells to be drilled.

Flow properties of a drilling fluid are strongly dependent on temperature and problems begin to occur when a critical temperature is reached. The effects are well known as well as the means to minimize some of these problems by additives. However temperature profiles, that could be encountered in a wellbore, must be carefully analyzed in order to treat a drilling fluid efficiently an economically.

Temperature in a wellbore is affected by frictional energy losses due to drillpipe contacting casing or borehole during rotation, viscous energy losses of the drilling fluid, frictional energy losses from the bit, energy loss of the cuttings and heat flow from the formation, which is the main problem. Different order of magnitude analyses [12, 14] demonstrated that other energy inputs are negligibly small. Approximation of formation heat flow is difficult and subject to many

different points of view. These views correspond to that many solutions, but existing models are considerably complex for actual field use.

CHAPTER 4

SCOPE

The scope of this study is to develop a simple empirical correlation to predict temperature profile of a drilling fluid in a circulating well. Using basic energy conservation principle, an exact solution is presented for a one dimensional system, in which the fluid is pumped to the drillpipe and collected from annulus, with multiple casing and cement segments. Since actual well testing is impossible for many different scenarios, experimental data is generated with a simulation created by using a commercial computer program that utilizes finite element method. The simulation and the analytic solution are used to collect data in different conditions. The results are compared with other studies. Statistical methods are used on the data collected from the simulator to obtain empirical correlations to simplify the analytical solution. Since the only parameter that would be important in the field is maximum temperature of the drilling fluid, an empirical correlation for estimating the maximum temperature is determined.

CHAPTER 5

THEORY

An analytical solution, similar to the solution of Kabir et al. [17] for estimating the temperature of a fluid flowing through a drillpipe and annulus as a function of depth and time is presented in this chapter. Since the problem has many variables, many assumptions were needed to simplify the equations for rapid implementation.

5.1. Assumptions

- Temperature of drilling fluid in a wellbore depends on many different heat input and output elements. These elements are listed below according to their effects in increasing order.

  a. Frictional energy losses due to drillpipe contacting casing or borehole during rotation
  b. Viscous energy losses of the drilling fluid
  c. Energy loss of the cuttings
  d. Frictional energy losses from the bit
  e. Heat flow from the formation.

Previous studies have shown [12, 14] that effects of a. to d. are small compared to that of e.. Heat flow from the formation is assumed to be the only heat source in this solution.

- The problem is reduced to one dimension by assuming no heat conduction in the axial direction. The heat is conducted only radial to the wellbore.
- Heat flow in the well bore is assumed to be steady state and heat flow in the formation is assumed to be transient.
- Viscosity and density of the flowing fluid is assumed to be constant with respect to changing temperature, and fluid is assumed to be incompressible. This assumption has not a big impact on the solution. As presented by Weintritt et al. [3] and Hiller [2], high pressure compensates for density and viscosity changes that are caused by high temperature to a degree.
- Fluid is assumed to be at constant temperature across the cross sections of drillpipe and annulus, thus axial temperature distribution is a straight line.
- Heat flow from the formation is assumed to be only conduction and approximated by an equation that utilizes Fourier's dimensionless temperature function [9, 17, 18].
- Heat transfer by radiation assumed to be nonexistent.
- Temperature of the fluid at the end of the drillpipe is assumed to be same with temperature of the fluid entering the annulus

5.2. Derivations

Expressions for annulus and drillpipe are obtained by setting up heat balance over the differential element of dx, demonstrated in figure 1. For the drillpipe element, heat enters system by convection ($\dot{Q}_p(x)$), conduction from annulus ($\dot{Q}_{ap}$), and leaves the system by convection ($\dot{Q}_{ap}(x+dx)$).

$$\dot{Q}_p(x+dx) - \dot{Q}_p(x) = \dot{Q}_{ap} \tag{1}$$

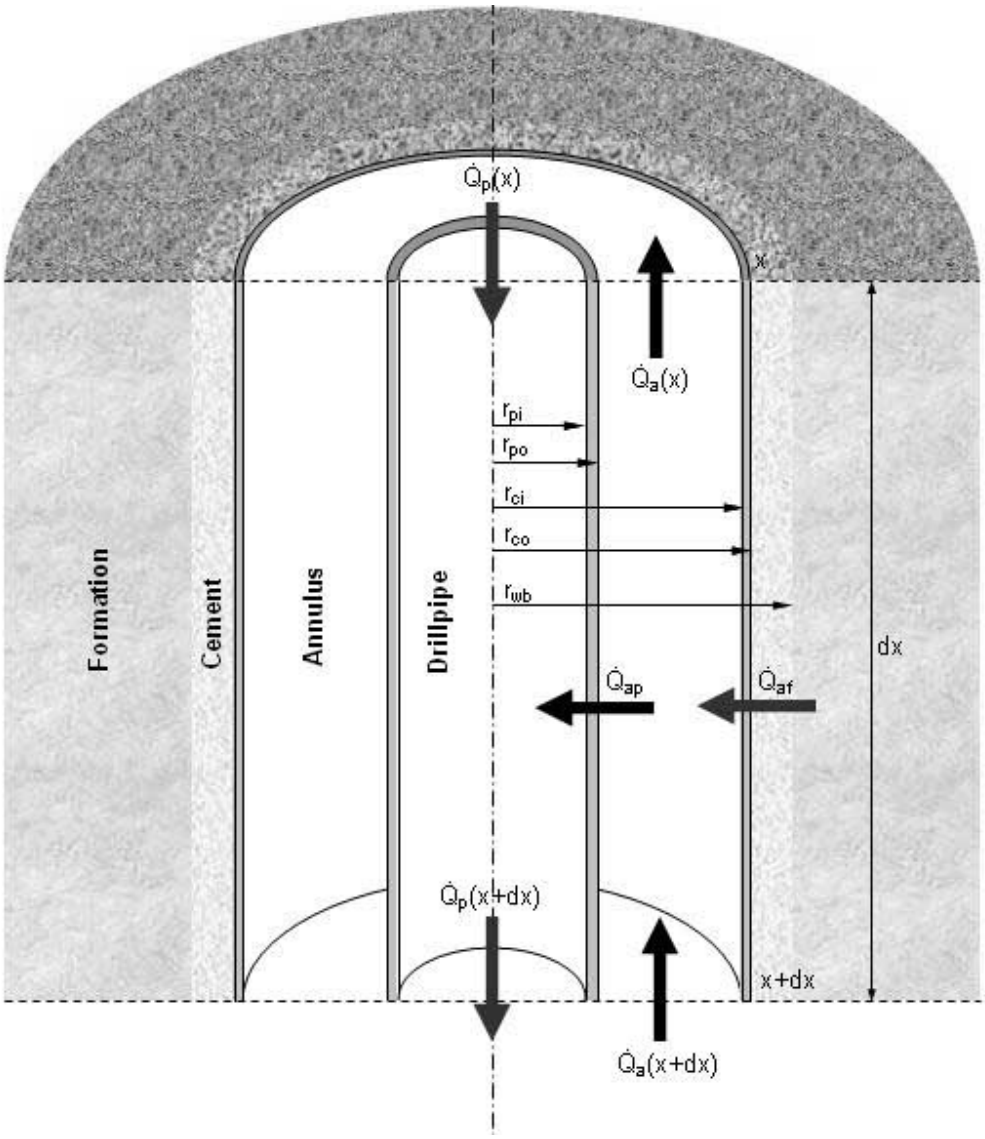

Figure 1. Diagram of the wellbore that has a length of dx.

Where heat accumulation in the drillpipe and heat flow across drillpipe are respectively given by,

$$\dot{Q}_p(x+dx)-\dot{Q}_p(x)=mc_p(T_{p(x+dx)}-T_{px}) \tag{2}$$

$$\dot{Q}_{ap}=2\pi r_{pi}U_p(T_a-T_p)dx \tag{3}$$

The equation (3) that gives heat flow from the annulus to drillpipe is an approximation, which utilizes overall heat transfer coefficient in drillpipe, U_p. It is used to define and combine the thermal resistances of different layers and could be adapted to any scenario [14, 21]. For the drillpipe, it is defined as,

$$\frac{1}{U_p}=\frac{1}{h_p}+\frac{r_{pi}}{k_p}Ln\left(\frac{r_{po}}{r_{pi}}\right)+\frac{r_{pi}}{r_{po}}\frac{1}{h_a} \tag{4}$$

First term depicts the heat transfer resistance of the thin film of drilling fluid inside the drillpipe at r_{pi}, second term is for thermal resistance of drillpipe and the third term defines the thermal resistance of the thin film of drilling fluid outside the drillpipe at r_{po}. To calculate coefficients of heat transfer for the drilling fluid in drillpipe and casing a simple relationship, defined in McAdams [20] is used,

$$\frac{h_p 2r_{pi}}{k}=0.023\left[N_{REp}\right]^{0.8}\left[N_{Pr}\right]^{0.4}=0.023\left[\frac{2m}{r_{pi}\mu}\right]^{0.8}\left[\frac{c_p\mu}{k}\right]^{0.4} \tag{5}$$

Substituting equations (2) and (3) into (1) yields,

$$mc_p(T_{px}-T_{p(x+dx)})=2\pi r_{pi}U_p(T_a-T_p)dx \tag{6}$$

$$\frac{dT_p}{dx} = \frac{2\pi r_{pi} U_p}{mc_p}(T_a - T_p) \tag{7}$$

Defining $\frac{2\pi r_{pi} U_p}{mc_p} = A$, and rewriting the equation (7),

$$\frac{dT_p}{dx} = AT_a - AT_p \tag{8}$$

For the annular element, heat enters system by convection ($\dot{Q}_a(x+dx)$), conduction from annulus ($\dot{Q}_{af}$), and leaves the system by convection ($\dot{Q}_{ap}(x)$) and conduction ($\dot{Q}_{ap}$).

$$\dot{Q}_a(x+dx) - \dot{Q}_a(x) = \dot{Q}_{ap} - \dot{Q}_{af} \tag{9}$$

Where heat accumulation in the annulus and heat flow across drillpipe are respectively given by,

$$\dot{Q}_a(x+dx) - \dot{Q}_a(x) = mc_p(T_{a(x+dx)} - T_{ax}) \tag{10}$$

$$\dot{Q}_{ap} = 2\pi r_{pi} U_p (T_a - T_p) dx \tag{3}$$

Approximation of formation heat flux is a somewhat complex process. Many authors [9-20] have concentrated on this problem and came up with different methods. The method used by Kabir et al. [17] will be employed in this study. Then heat flow from the formation to the wellbore is,

$$\dot{Q}_{af} = \frac{2\pi k_f}{T_D}(T_f - T_{wb}) dx \tag{11}$$

T_D, Fourrier's dimensionless temperature function, in equation (11) is used to approximate formation cool down effect with time [9, 17, 18, 20, 21]. Formulation of Hasan et al. [22] is adapted in this study.

$$T_D = \left(1.1281\sqrt{t_D}\right)\times\left(1-0.3\sqrt{t_D}\right) \qquad \text{if } 10^{-10} \le t_D \le 1.5 \tag{12}$$

$$T_D = \left(0.4063+0.5\ln t_D\right)\times\left(1+\frac{0.6}{t_D}\right) \qquad \text{if } t_D > 1.5 \tag{13}$$

Where,

$$t_D = \frac{\alpha t}{r_{wb}} \qquad \text{and} \qquad \alpha = \frac{k_f}{c_f \rho_f}$$

Following Heat is transferred from the wellbore through possible cement and casing layers to annulus. According to Holmes and Swift [10], the equation for this relationship is given as,

$$\dot{Q} = 2\pi r_{ci} U_a (T_{wb} - T_a) dx \tag{14}$$

Assuming these heat fluxes are equal, temperature at formation-wellbore interface, T_{wb} could be eliminated.

$$\dot{Q}_{af} = \dot{Q} = \frac{2\pi k_f}{T_D}(T_f - T_{wb})dx = 2\pi r_{ci} U_a (T_{wb} - T_a) dx \tag{15}$$

$$\dot{Q} - \dot{Q}_{af} = 2\pi r_{ci} U_a (T_{wb} - T_a) dx - \frac{2\pi k_f}{T_D}(T_f - T_{wb})dx = 0 \tag{16}$$

$$r_{ci} U_a T_D (T_{wb} - T_a) - k_f (T_f - T_{wb}) = 0 \tag{17}$$

$$T_{wb}(k_f + r_{ci}U_aT_D) = k_fT_f + r_{ci}U_aT_DT_a \tag{18}$$

Substituting equation (18) into equation (11) and simplifying yields,

$$\dot{Q}_{af} = \frac{2\pi k_f}{T_D}\left(T_f - \frac{k_fT_f + r_{ci}U_aT_DT_a}{k_f + r_{ci}U_aT_D}\right)dx \tag{19}$$

$$\dot{Q}_{af} = \frac{2\pi k_f}{T_D}\left(\frac{k_fT_f + r_{ci}U_aT_DT_f - k_fT_f - r_{ci}U_aT_DT_a}{k_f + r_{ci}U_aT_D}\right)dx \tag{20}$$

$$\dot{Q}_{af} = \frac{2\pi r_{ci}U_ak_f}{k_f + r_{ci}U_aT_D}\left(T_f - T_a\right)dx \tag{21}$$

The heat balance on the annular element, equation (9) becomes,

$$mc_p(T_{a(x+dx)} - T_{ax}) = 2\pi r_{pi}U_p(T_a - T_p)dx - \frac{2\pi r_{ci}U_ak_f}{k_f + r_{ci}U_aT_D}\left(T_f - T_a\right)dx \tag{22}$$

$$\frac{dT_a}{dx} = \frac{2\pi r_{pi}U_p}{mc_p}(T_a - T_p) - \frac{2\pi r_{ci}U_ak_f}{mc_p\left(k_f + r_{ci}U_aT_D\right)}\left(T_f - T_a\right) \tag{23}$$

Defining $\frac{2\pi r_{ci}U_ak_f}{mc_p\left(k_f + r_{ci}U_aT_D\right)} = B$, and rewriting the equation (23),

$$\frac{dT_a}{dx} = A(T_a - T_p) - B\left(T_f - T_a\right) \tag{24}$$

With equations (8) and (24), two unknowns, namely T_a and T_p could be determined. The equation (8) is rewritten and substituted into equation (24) as,

$$T_a = \frac{1}{A}\frac{dT_p}{dx} + T_p \tag{25}$$

$$\frac{d}{dx}\left(\frac{1}{A}\frac{dT_p}{dx} + T_p\right) = A\left(\left[\frac{1}{A}\frac{dT_p}{dx} + T_p\right] - T_p\right) - B\left(T_f - \left[\frac{1}{A}\frac{dT_p}{dx} + T_p\right]\right) \tag{26}$$

$$\frac{1}{A}\frac{d^2T_p}{dx^2} + \frac{dT_p}{dx} = \frac{dT_p}{dx} + AT_p - AT_p - BT_f + \frac{B}{A}\frac{dT_p}{dx} + BT_p \tag{27}$$

$$\frac{1}{A}\frac{d^2T_p}{dx^2} = \frac{B}{A}\frac{dT_p}{dx} + BT_p - BT_f \tag{28}$$

Formation temperature, T_f is often defined as a function of surface temperature, geothermal gradient and depth. Substituting $T_s + Gx$ into T_f and simplifying equation (28) yields,

$$\frac{d^2T_p}{dx^2} - B\frac{dT_p}{dx} - ABT_p = -AB\left(T_s + Gx\right) \tag{29}$$

Equation (29) is a nonhomogenous, second order and linear differential equation, and could be rewritten as,

$$\frac{d^2T_p}{dx^2} - B\frac{dT_p}{dx} - ABT_p = -AB\left(T_s + Gx\right) = f\left(x\right) \tag{30}$$

$$f\left(x\right) = -AB\left(T_s + Gx\right) \tag{31}$$

Particular solution for equation (30) is in the form of,

$$T_{pp} = \alpha x + \beta \tag{32}$$

Substituting equation (32) into (30) yields,

$$\frac{d^2(\alpha x + \beta)}{dx^2} - B\frac{d(\alpha x + \beta)}{dx} - AB(\alpha x + \beta) = -AB(T_s + Gx) \tag{33}$$

$$-B\alpha - AB(\alpha x + \beta) = -AB(T_s + Gx) \tag{34}$$

$$\frac{\alpha}{A} + \alpha x + \beta = T_s + Gx \tag{35}$$

$$(\alpha - G)x + \frac{\alpha}{A} + \beta - T_s = 0 \tag{36}$$

Coefficient of x and the other constants must be equal to 0, then,

$$\alpha = G \tag{37}$$

$$\beta = T_s - \frac{G}{A} \tag{38}$$

Substituting equations (37) and (38) into (32) gives the particular solution,

$$T_{pp} = Gx + T_s - \frac{G}{A} \tag{39}$$

Homogenous part of the equation (30) is,

$$\frac{d^2T_p}{dx^2} - B\frac{dT_p}{dx} - ABT_p = 0 \tag{40}$$

The auxiliary polynomial equation of (40) is,

$$\theta^2 - B\theta - AB = 0 \tag{41}$$

Equation (41) has the following roots,

$$\theta_1 = \frac{B + \sqrt{B^2 + 4AB}}{2} \tag{42}$$

$$\theta_2 = \frac{B - \sqrt{B^2 + 4AB}}{2} \tag{43}$$

Then the complementary solution is,

$$T_{pc} = C_1 e^{\theta_1 x} + C_2 e^{\theta_2 x} \tag{45}$$

Finally, by substituting equations (39) and (45) into (30) gives the temperature distribution in the drillpipe,

$$T_p = C_1 e^{\theta_1 x} + C_2 e^{\theta_2 x} + Gx + T_s - \frac{G}{A} \tag{46}$$

To calculate the temperature distribution in annulus, equation (46) is substituted in equation (8),

$$T_a = \frac{1}{A}\frac{d}{dx}\left(C_1 e^{\theta_1 x} + C_2 e^{\theta_2 x} + Gx + T_s - \frac{G}{A}\right) + \left(C_1 e^{\theta_1 x} + C_2 e^{\theta_2 x} + Gx + T_s - \frac{G}{A}\right) \tag{47}$$

$$T_a = \frac{1}{A}\left(\theta_1 C_1 e^{\theta_1 x} + \theta_2 C_2 e^{\theta_2 x} + G\right) + C_1 e^{\theta_1 x} + C_2 e^{\theta_2 x} + Gx + T_s - \frac{G}{A} \tag{48}$$

$$T_a = \left(1+\frac{\theta_1}{A}\right)C_1 e^{\theta_1 x} + \left(1+\frac{\theta_2}{A}\right)C_2 e^{\theta_2 x} + Gx + T_s \tag{49}$$

In order to calculate the integration constants C_1 and C_2, boundary conditions are used. At the wellhead, $x = 0$, temperature in the drillpipe is equal to inlet temperature, $T_p = T_{pi}$, then equation (46) becomes,

$$T_{pi} = C_1 + C_2 + T_s - \frac{G}{A} \tag{50}$$

At the bottomhole, $x = H$, temperatures in the annulus and in the drillpipe are equal, $T_a = T_p$, then,

$$C_1 e^{\theta_1 H} + C_2 e^{\theta_2 H} + GH + T_s - \frac{G}{A} = \left(1+\frac{\theta_1}{A}\right)C_1 e^{\theta_1 H} + \left(1+\frac{\theta_2}{A}\right)C_2 e^{\theta_2 H} + GH + T_s \tag{51}$$

$$\left(1+\frac{\theta_1}{A}-1\right)C_1 e^{\theta_1 H} + \left(1+\frac{\theta_2}{A}-1\right)C_2 e^{\theta_2 H} + \frac{G}{A} = 0 \tag{52}$$

$$\theta_1 C_1 e^{\theta_1 H} + \theta_2 C_2 e^{\theta_2 H} + G = 0 \tag{53}$$

Substituting equation (50) in the form of $C_2 = T_{pi} - C_1 - T_s + \frac{G}{A}$ into equation (53) yields,

$$\theta_1 C_1 e^{\theta_1 H} + \theta_2 \left(T_{pi} - C_1 - T_s + \frac{G}{A}\right) e^{\theta_2 H} + G = 0 \tag{54}$$

$$C_1 \theta_1 e^{\theta_1 H} + \left(T_{pi} - T_s + \frac{G}{A}\right)\theta_2 e^{\theta_2 H} - C_1 \theta_2 e^{\theta_2 H} + G = 0 \tag{55}$$

$$C_1\left(\theta_1 e^{\theta_1 H}-\theta_2 e^{\theta_2 H}\right)=\left(T_{pi}-T_s+\frac{G}{A}\right)\theta_2 e^{\theta_2 H}-G \tag{56}$$

$$C_1=\frac{\left(T_{pi}-T_s+\frac{G}{A}\right)\theta_2 e^{\theta_2 H}-G}{\left(\theta_1 e^{\theta_1 H}-\theta_2 e^{\theta_2 H}\right)} \tag{57}$$

Similarly, substituting equation (50) in the form of $C_1=T_{pi}-C_2-T_s+\frac{G}{A}$ into equation (53) yields,

$$\theta_1\left(T_{pi}-C_2-T_s+\frac{G}{A}\right)e^{\theta_1 H}+\theta_2 C_2 e^{\theta_2 H}+G=0 \tag{58}$$

$$\left(T_{pi}-T_s+\frac{G}{A}\right)\theta_1 e^{\theta_1 H}-C_2\theta_1 e^{\theta_1 H}+C_2\theta_2 e^{\theta_2 H}+G=0 \tag{59}$$

$$C_2\left(\theta_1 e^{\theta_1 H}-\theta_2 e^{\theta_2 H}\right)=\left(T_{pi}-T_s+\frac{G}{A}\right)\theta_1 e^{\theta_1 H}-G \tag{60}$$

$$C_2=\frac{\left(T_{pi}-T_s+\frac{G}{A}\right)\theta_1 e^{\theta_1 H}-G}{\left(\theta_1 e^{\theta_1 H}-\theta_2 e^{\theta_2 H}\right)} \tag{61}$$

5.3. Application of the Equations to Casing and Cement Layers

This application depends on formulating the thermal resistances of different layers of casing and cement as demonstrated in figure 2. Overall heat transfer coefficient for the annulus, U_a is employed for this task. Different forms of this coefficient are used by many authors [9, 10, 11, 14, 17, 18, 21, 22]. Following general formulation is used in this study,

$$\frac{1}{U_a} = \frac{1}{h_a} + \frac{r_{cin}}{k_{pn}} Ln\left(\frac{r_{con}}{r_{cin}}\right) + \frac{r_{cin}}{k_{en}} Ln\left(\frac{r_{ci(n-1)}}{r_{cin}}\right) + \ldots + \frac{r_{ci1}}{k_{p1}} Ln\left(\frac{r_{co1}}{r_{ci1}}\right) + \frac{r_{ci1}}{k_{e1}} Ln\left(\frac{r_{wb}}{r_{co1}}\right) \quad (62)$$

The terms in the equation can be listed as follows,

- $\frac{1}{h_a}$: is used for thermal resistance of the thin film of drilling fluid at r_{ci1}.
- $\frac{r_{ci1}}{k_{p1}} Ln\left(\frac{r_{co1}}{r_{ci1}}\right)$: is used for thermal resistance of the casing layer 1.
- $\frac{r_{ci1}}{k_{e1}} Ln\left(\frac{r_{ci2}}{r_{co1}}\right)$: is used for thermal resistance of cement layer 1.
- $\frac{r_{cin}}{k_{pn}} Ln\left(\frac{r_{con}}{r_{cin}}\right)$: is used for thermal resistance of the casing layer n (last layer).

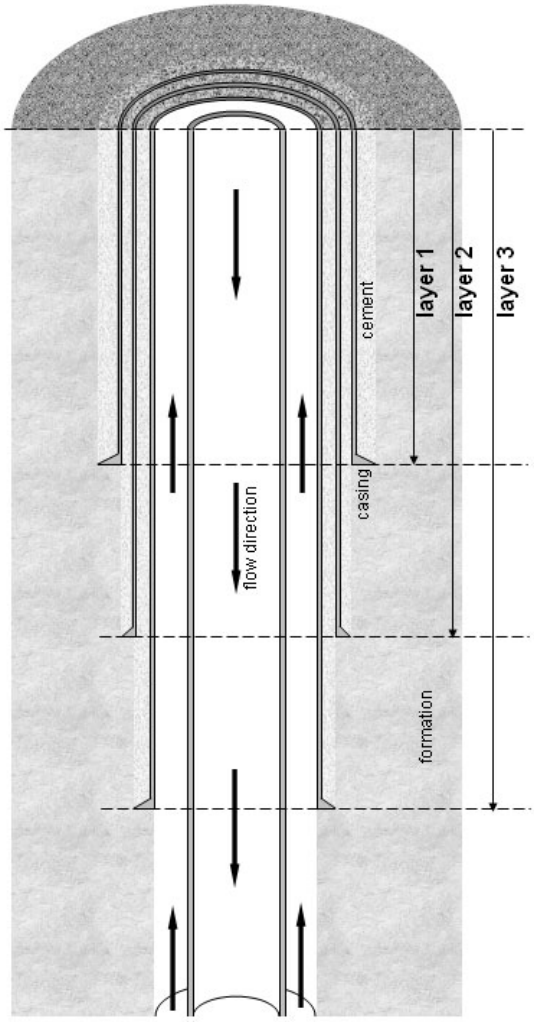

Figure 2. Different casing and cement layers in a wellbore

- $\frac{r_{cin}}{k_{en}} Ln\left(\frac{r_{wb}}{r_{cin}}\right)$: is used for thermal resistance of cement layer n (last layer.

In the case of openhole segments, neglecting the thermal resistance of drilling fluid cake, the equation would simplify to:

$$\frac{1}{U_a} = \frac{1}{h_a} \tag{63}$$

CHAPTER 6

COMPUTER WORK

Experimental data is required in order to verify the analytical model and obtain more data on maximum drilling fluid temperature in a circulating well. A commercial computer program, ANSYS is used for this purpose. Different wells with different drilling fluid properties are simulated. Main focus of this part of the study is to obtain maximum drilling fluid temperature for different variables.

In order to obtain the results more rapidly, a two dimensional model was constructed. Since modeling took a considerable amount of time, same well geometry was used in three different depth arbitrarily chosen configurations, which are namely 1640 ft, 3280 ft and 4920 ft. Modeling deeper wells were not feasible, due to very long computation time and limitations of the program. For simplicity, no casing strings and altered zones were added to the model. To observe the formation cool-down effect, three blocks of rock were modeled around the well. Rock adjacent to the well from both sides was 164 ft and block of rock underlying these was 328 ft. Figure 3 shows the different elements and geometry used in 1640 ft model.

Since the temperature profile was sought in a dynamic fluid body, the best choice was to employ FLOTRAN CFD discipline of ANSYS. The formation and the well were assumed to be cylindrical, thus a 2D cross sectional model of

the system was deemed an accurate representation. Quadrilateral element with four nodes, which has fluid velocity, pressure, temperature, turbulent kinetic energy, turbulent energy dissipation, multiple species mass fractions as degrees of freedom was used for 2D FLOTRAN CFD analysis. Three materials were defined. FLOTRAN CFD used the first material (material 0) as the fluid, and the others as the solids.

Models were meshed for keeping the node number at a minimum while maintaining a good degree of accuracy. Achieving this degree required considerable amount of experimenting and time. Unstructured mesh, which used extensive computation time, was a serious problem for the dimensions of these models, so the geometry was redesigned to accommodate structured meshing. Different mesh sizes were tried, starting from 1ft x 1ft. Since temperature change on both axes was considerably slow, mesh size of the formation was selected to be 16. 4 ft x 32.8 ft. The vertical mesh size also remained 32.8 ft for the well, but horizontally all the conduits and pipes were meshed to have at least 3 nodes. The nodes in the formation of the 1640 ft model could be seen as white dots in the figure 3, and meshing of the bottom of the well can be seen in the figure 4. Additionally, 1640 ft model had 2079 nodes; 3280 ft model had 3729 nodes and 4920 ft model had 5379 nodes.

After meshing the models, loads were defined for the analyses. Fluid flow was managed by calculating the maximum velocity of the fluid in the pipe from the given flow rate and defining this value at the entrance of the drilling fluid as a negative fluid flow load in negative y direction, defining the pressure at annular exit points to be zero, and defining a 0 velocity at drill pipe and annulus lines. Initial temperature of the fluid was also given at the drill pipe entry as a temperature load.

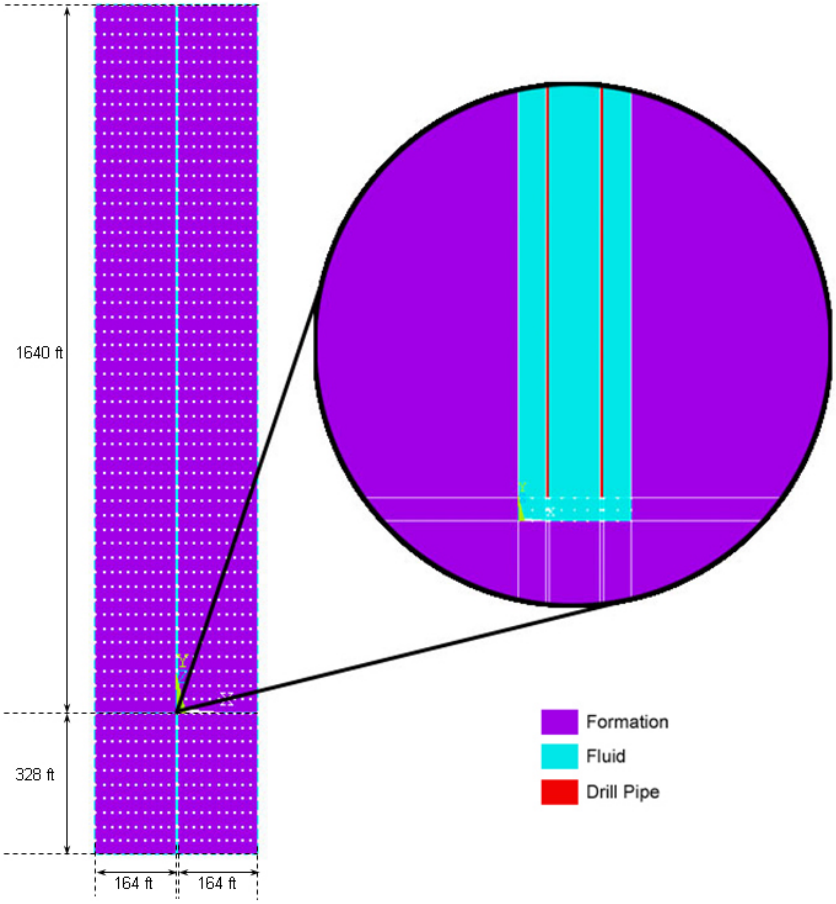

Figure 3. Element view of the 1640 ft model.

A partial wellbore geometry was modeled with the dimensions shown in figure 4.

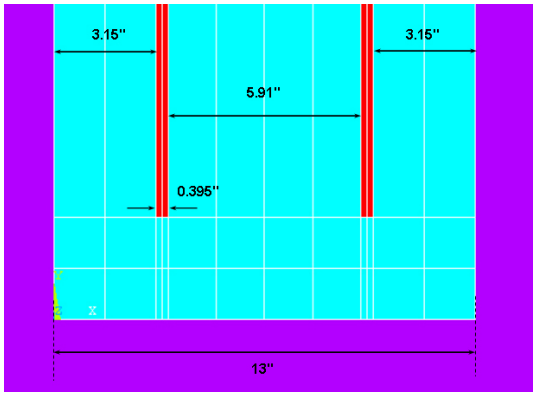

Figure 4. Wellbore geometry at the bottom.

Two relatively high geothermal gradients, which are 3.65 ^{o}F/100ft and 6.85 ^{o}F/100ft were used. Temperature change with respect to depth was formed in the model by solving it with constant temperature loads at surface and at the bottom of the underlying rock block at steady state condition. The heat transfer is assumed to be only in the form of conduction and is from earth's core to the surface. With this method, it was possible to observe two dimensional heat conduction in the formation. An example of the linear gradient achieved by this method is demonstrated in Figure 5.

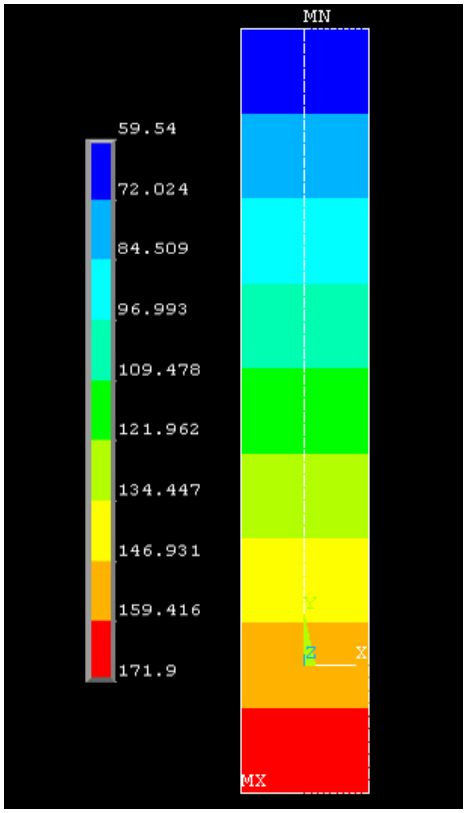

Figure 5. Change of temperature with respect to depth in the 1640 ft model.

After establishing the procedure for generating the temperature change with respect to depth, different solutions were made by changing flow rate, time, geothermal gradient, formation specific heat, formation conductivity, fluid inlet temperature and surface earth temperature. A sample simulation run is given in Appendix D.

Over 10000 data points were collected. Results of each simulation run were carefully analyzed and checked. Faulty runs were remade. All data was then listed and transferred to a commercial statistical analysis program. Simple correlations that could easily be used in the field were sought. The first correlation was for the temperature profile in the pipe and annulus. Dimensional analysis was done for the variables. But the resulting equation had a very high error margin. After careful analysis of the data at hand, several variables that presented little significance in their possible window of change, namely fluid and formation specific heat and conductivity, pipe and annulus diameter, formation density, fluid density and viscosity. Rigorous trials were made with the variables at hand to match a formula to the temperature profile data. Following correlation was the one with the smallest average error of 15.5 %.

$$T_p = T_{pi} - 0.3207t + 0.0465x + 1193.651G - 0.0166q - 1.0401T_s \qquad (1)$$

$$T_a = T_p - 0.00945t + 0.000006x + 47.869G + 0.00387q - 0.05112T_s \qquad (2)$$

These formulas are easy to use and easily implemented to have an idea about the temperature profile. The main objective of simulations was to obtain a correlation for the maximum temperature inside the wellbore. Similarly dimensionless groups were developed for this task, but error was too high, so same variables were used to achieve a simple correlation.

$$T_{\max} = 0.7238(t)^{-0.0488}(x)^{0.8153}(G)^{0.7279}(q)^{-0.0879}(T_i)^{0.0857}(T_s)^{0.3622} \qquad (3)$$

Equation (3) has an average error of 6.7 %. In field terms this margin is acceptable.

CHAPTER 7

RESULTS AND DISCUSSION

A spreadsheet program was developed and used to obtain solutions for temperature profile behavior within the drillstring and wellbore as a function of time and circulation rate, and effects of different casing and cement layers. Maximum temperature inside the well is observed. The finite element computer simulation was run for different scenarios and compared with the results obtained from the analytical solution.

7.1. Results from Analytical Solution

In order to check the validity of the solution, steady state solution of Holmes and Swift [9], which is presented in appendix A, is employed. Figure 6 presents such comparison. In order to see the effect of heat transfer from the formation when steady state condition is reached, a circulation time of 1000 hours had to be assumed. Both of the models are predicting the temperature profile at steady state conditions virtually identically. However, when the circulation time variable is taken into account, Holmes and Swift [10] model actually fails to predict correctly as seen in figure 7. In fact, the transient calculation of Holmes and Swift [10] are showing a poor performance when compared with computer simulation results. The maximum temperature difference is about 14 ^{o}F, which

is significantly high for an approximation to be accepted as accurate. Sample calculation procedures for the model used in this study are given in Appendix B and C.

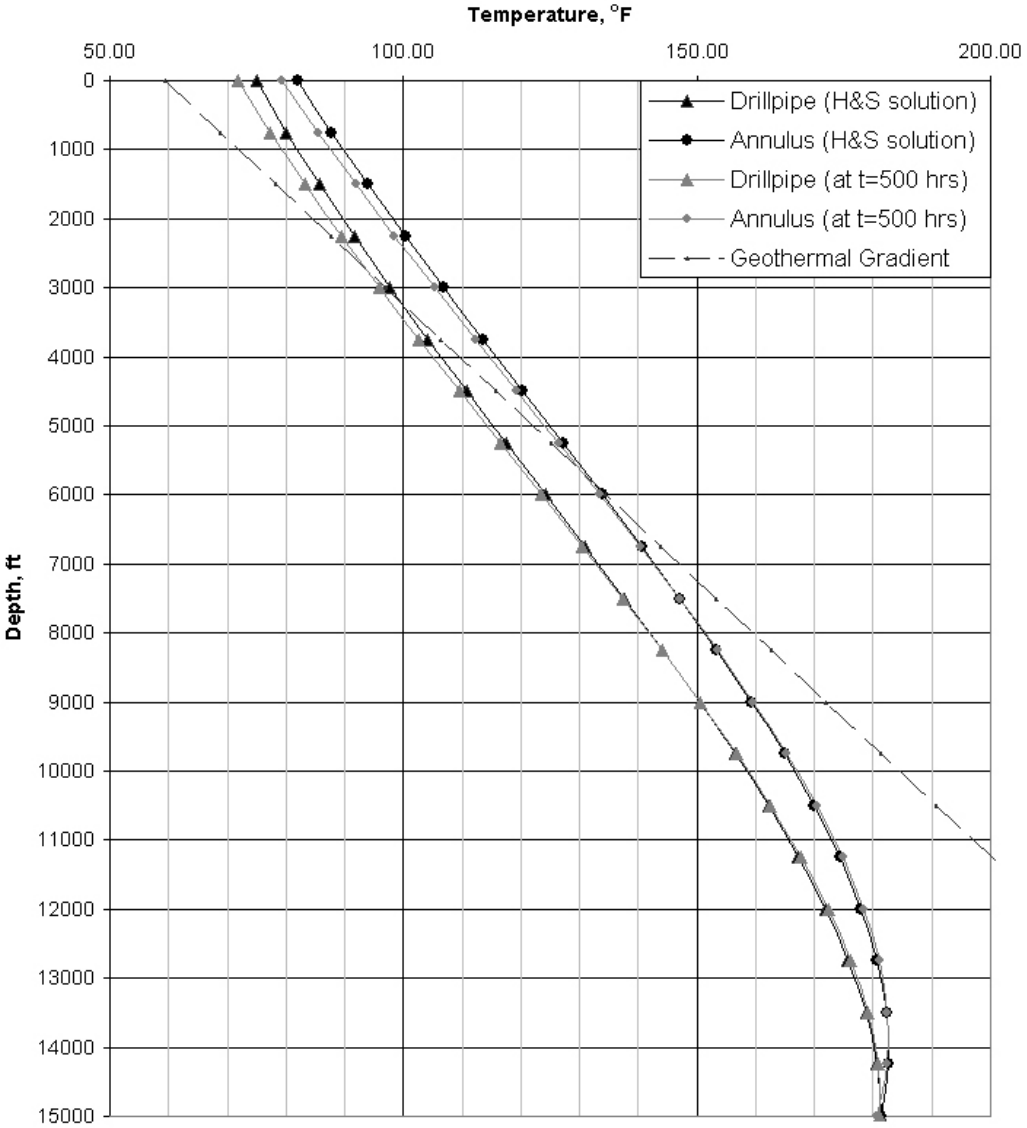

Figure 6. Temperature profile comparison with Holmes and Swift [9] Model

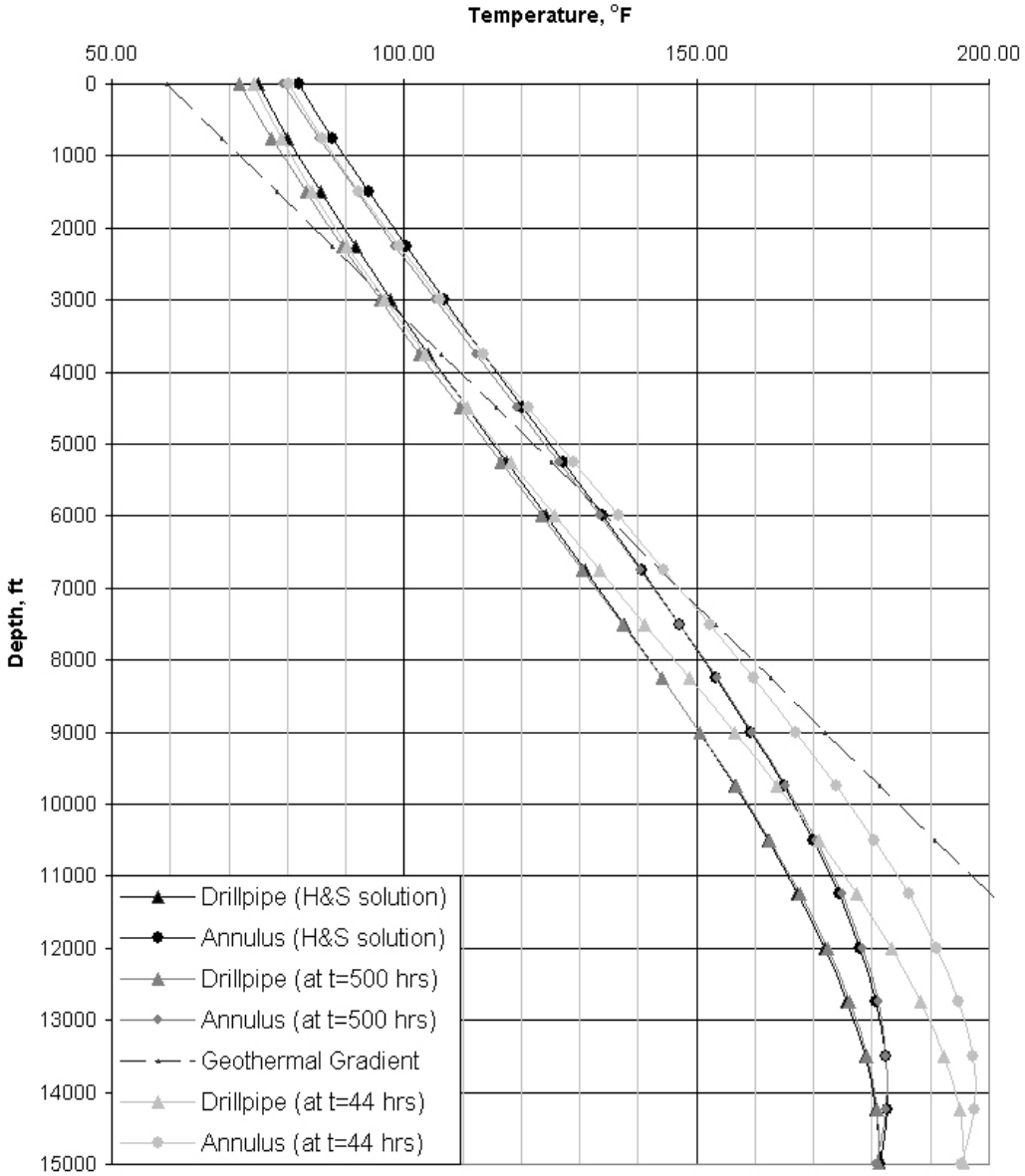

Figure 7. Temperature profile comparison with Holmes and Swift [9] Model

Further analysis of the model reveals the dependence of temperature profile and maximum fluid temperature on different variables. Well and drilling fluid data from Holmes and Swift [10] are used generating the charts below, which is given in table 1. Only one variable is changed during this sensitivity analysis. Effect of circulation rate for t=44 hr has been presented in figure 8. It can be clearly observed that as the flow rate is increased, the heat transfer on the drilling fluid is relieved, thus, the maximum drilling fluid temperature within the wellbore reduces significantly.

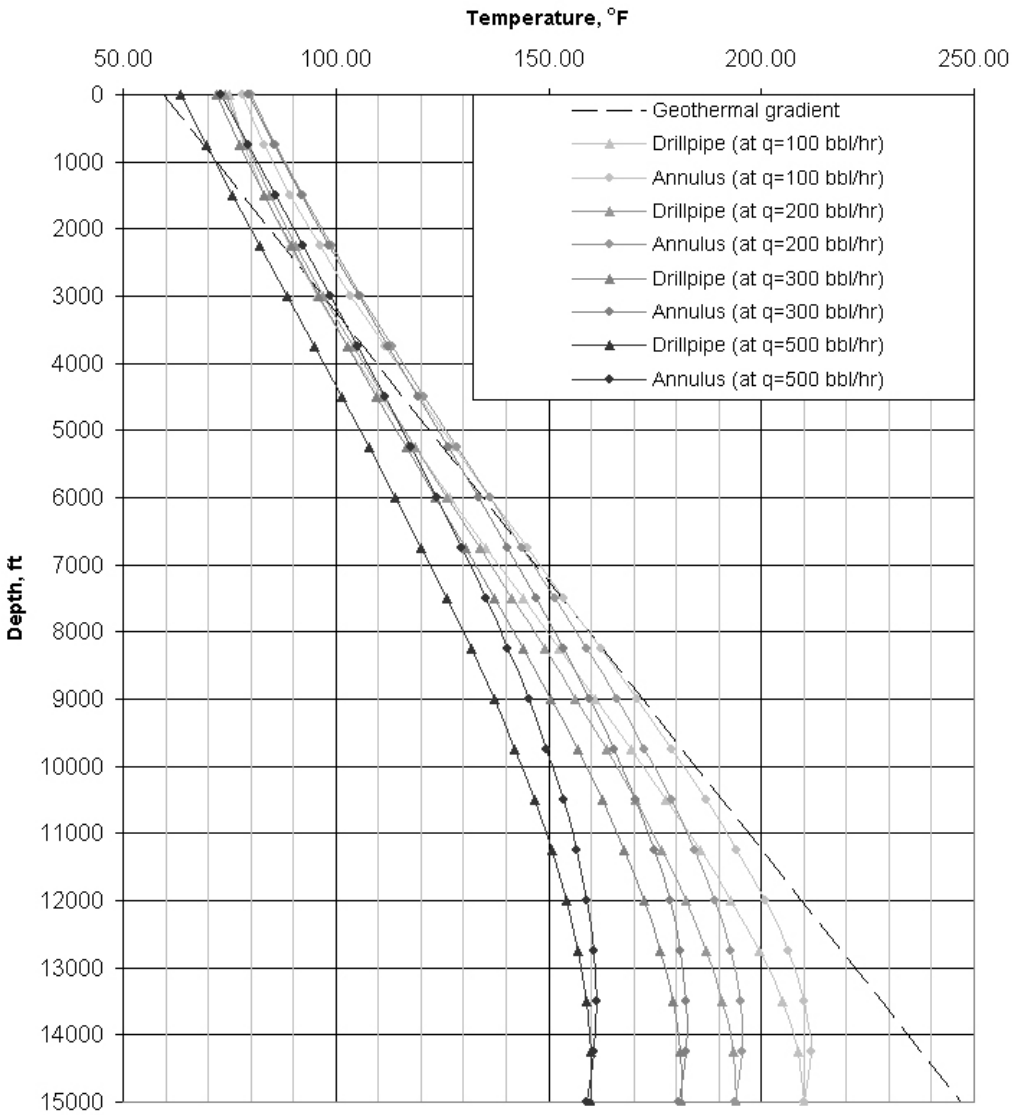

Figure 8. Change of temperature profile with different flow rates

Since the significant parameter that is sought for is the maximum temperature, different values of it could be calculated with varying pump rate and time. Figure 9 clearly demonstrates that the maximum temperature decreased as the flow rate increased with a nearly linear profile.

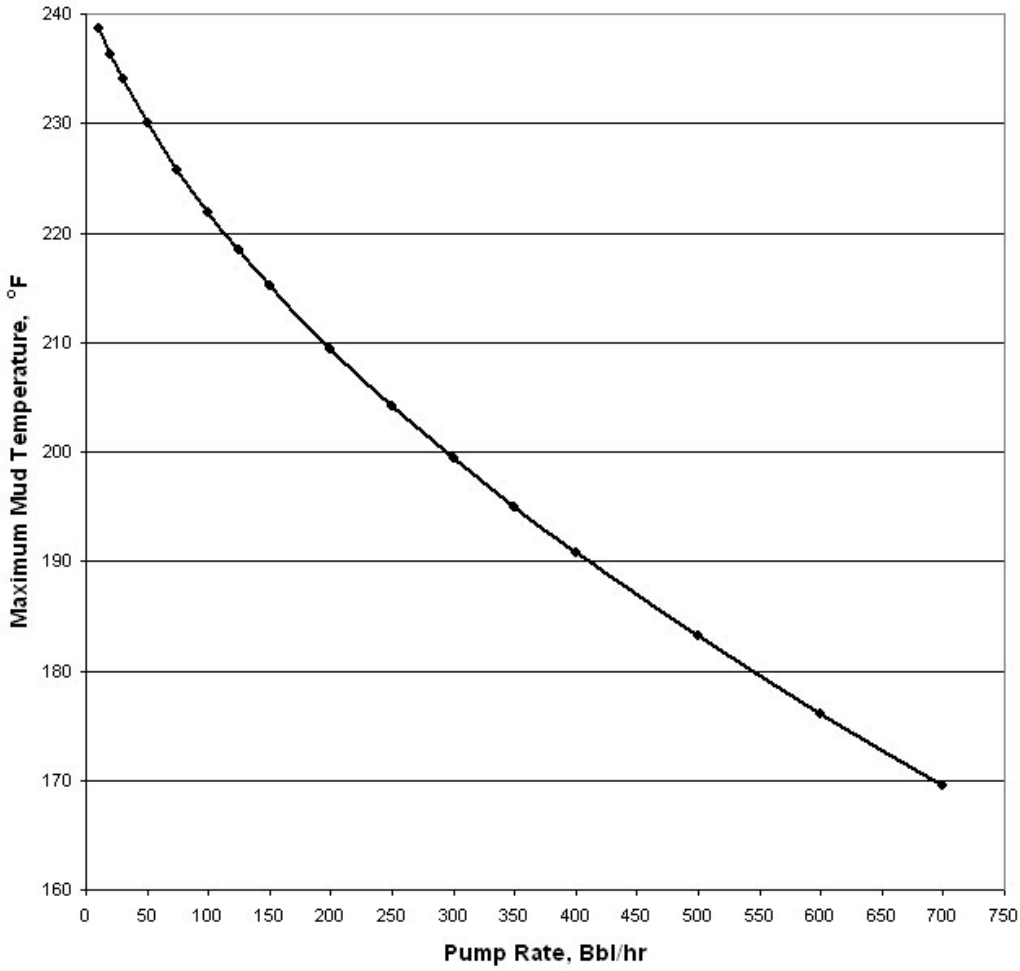

Figure 9. Change of maximum temperature with pump rate

For different circulation times, temperature profile change is presented in figure 10. Formation cool-down effect can clearly be observed with increasing time. As the temperature difference between the formation and fluid in the annulus decreased, temperature profile lines in both conduits shifted left, signifying a drop in overall temperature.

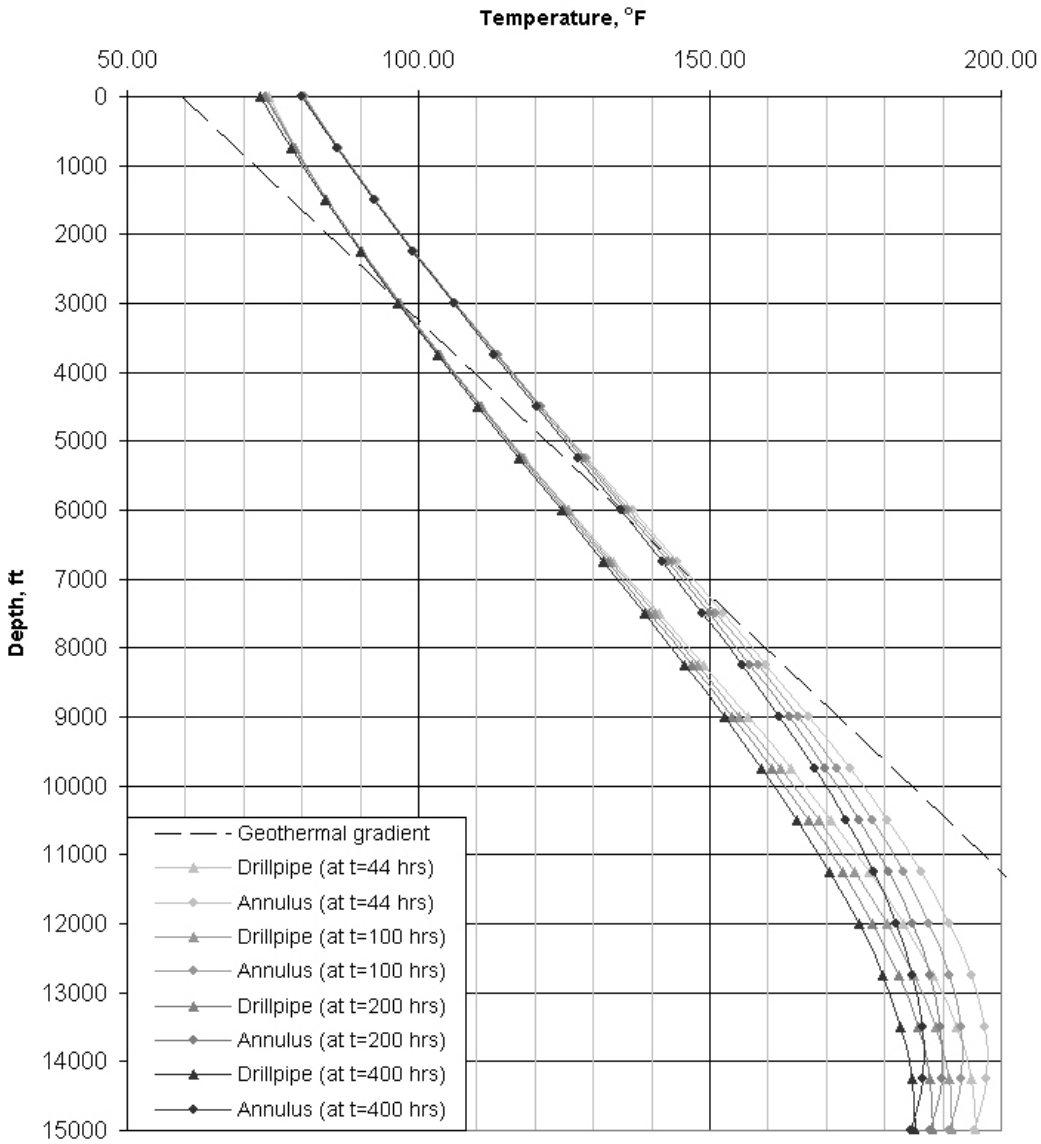

Figure 10. Change of temperature profile with different circulation time

Similarly, maximum temperature change with increasing circulation time was analyzed. As it can be seen in the Figure 11, the most significant change in maximum temperature occurs in early time, and later it begins its slow and linear approach to geothermal gradient.

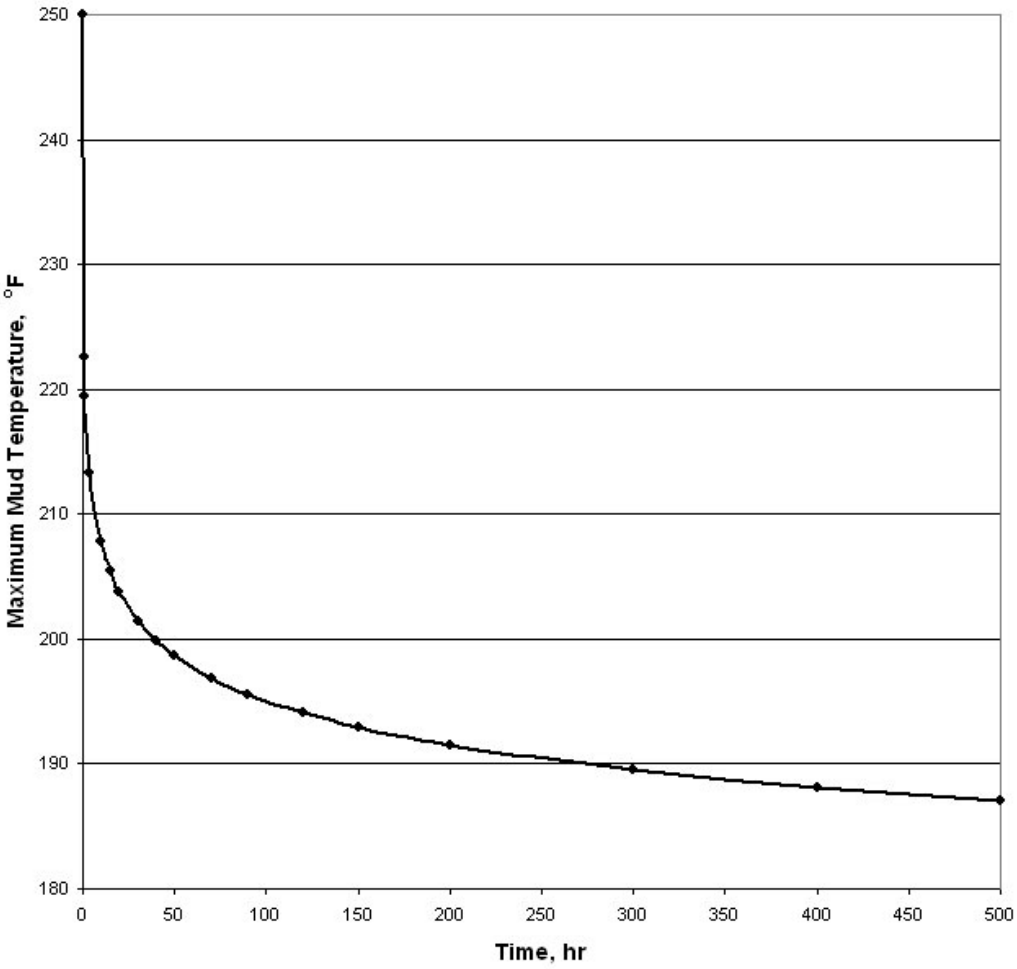

Figure 11. Change of maximum temperature with circulation time

Application of the model to a series of casing string demonstrated in figure 2 is presented in figure 12. As it can be seen, effects of different casing layers to the maximum temperature of the fluid are insignificant. Both solutions were carried out with same set of variables and the temperature difference was less than 2°F. A sample calculation is available in Appendix C.

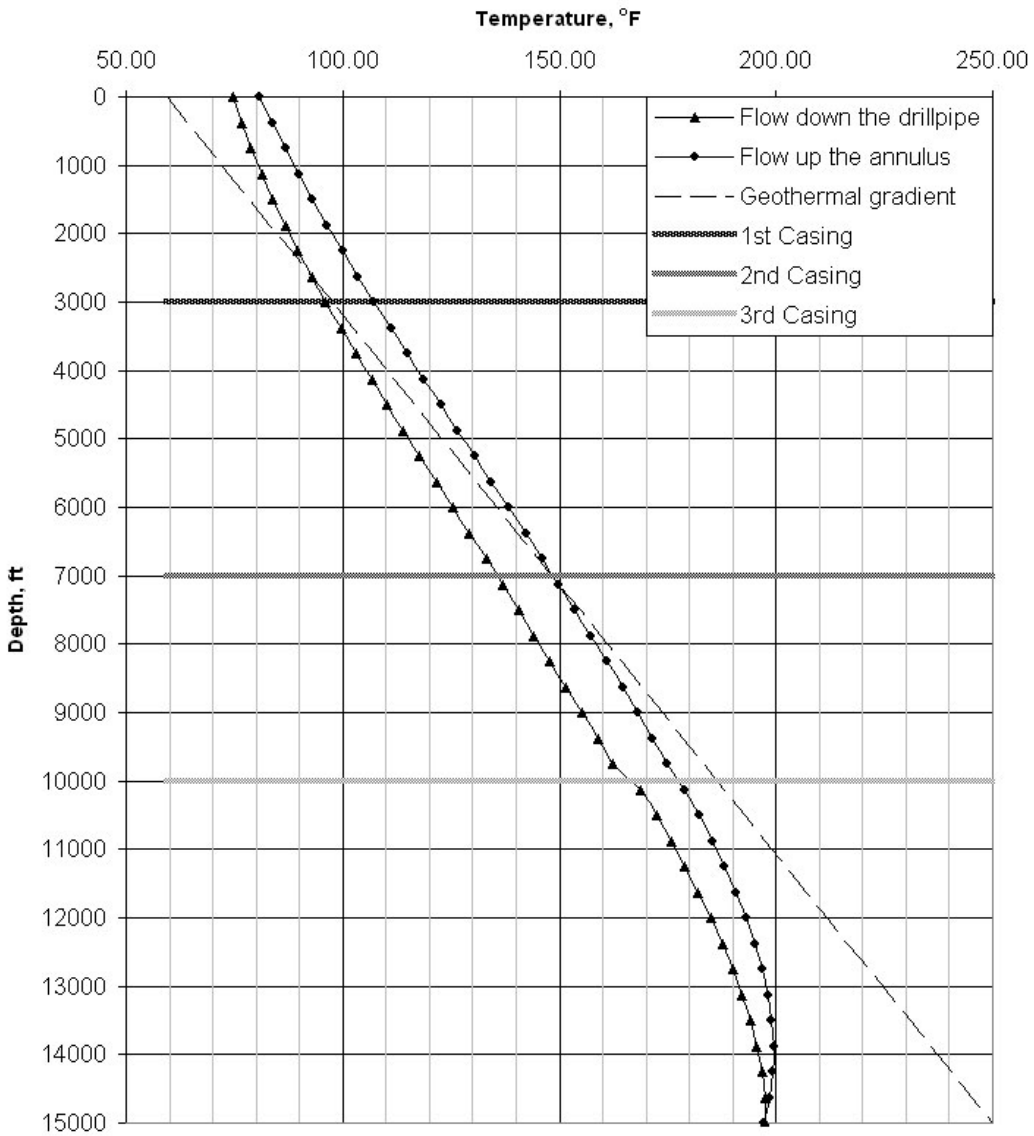

Figure 12. Temperature distribution in a well with casing strings.

The important drawback of the analytical method is that results become unreliable when the depth has a value below 12000 ft, i.e., the analytical method works properly above a certain depth. Below 12000 ft, the model starts calculating the fluid inlet temperature below the original assigned value, and a discontinuity develops at the bottomhole. Thus, the rest of the data points become bogus. Below is the case that is solved by using Holmes and Swift [10] data except the depth of the well, which taken as 5000 ft. The given pipe inlet temperature was 75°F, but it is calculated as 58°F.

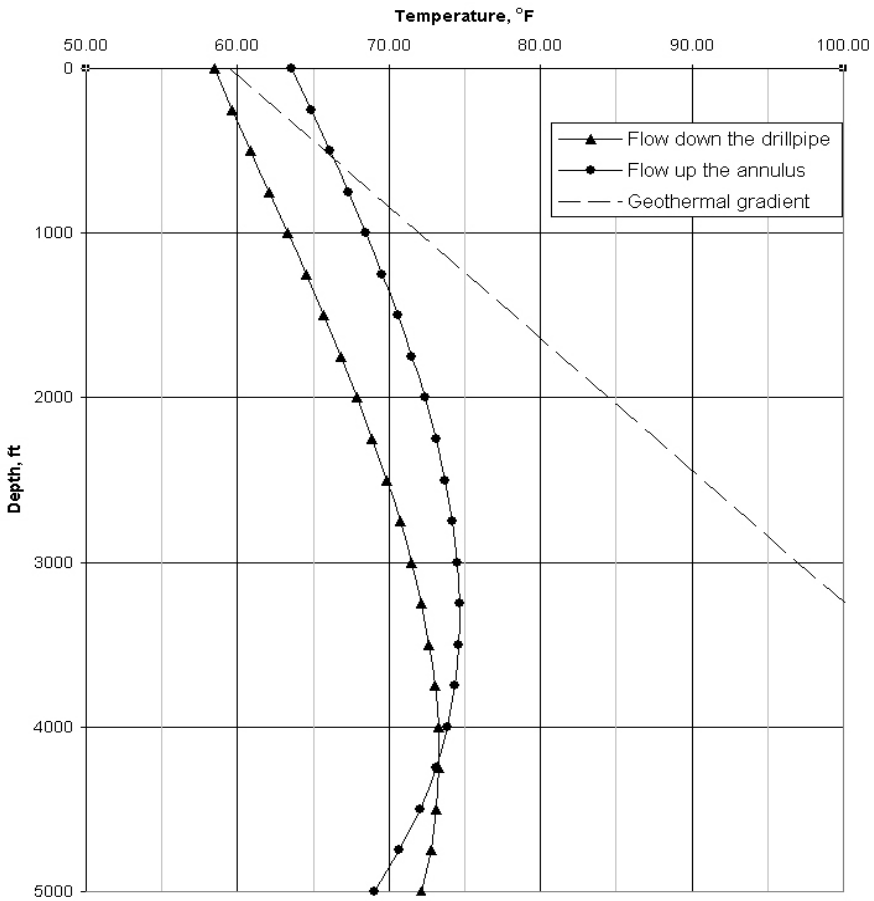

Figure 13. Temperature distribution in a 5000 ft well.

Considerable amount of recalculation and rechecking were done on the resulting equations, but no error was found in the calculation. It could be speculated that the analytic solution inherits an error due to the dependence of temperature in both drill pipe and annulus to each other.

7.2. Results from Computer Work

Each simulation was run for transient analysis. A total of 37.5 hours, 15 time steps with each step length of 2.5 hours of continuous circulation was implemented. It has been observed that after 37.5 hrs, steady state conditions are almost reached. Data was then collected from points in both annulus and drill pipe with sufficient length intervals. Temperature distribution correlation and maximum temperature correlation data was obtained with relatively less effort once the variables were listed in a spreadsheet program.

7.2.1. Simulation Data

Six different flow rates, namely 75 bbl/hr, 125 bbl/hr, 225 bbl/hr, 500 bbl/hr, 1000 bbl/hr and 1500 bbl/hr, were used with three different wells. Since first three flow rates are relatively small, they had a little impact on shifting the temperature distribution lines away from geothermal gradient line. Therefore, main emphasis was on the last three flow rates, while presenting the results.

The 1640 ft. well was the one that had the most diverse analysis. Apart from flow rate changes, effects of formation specific heat and conductivity, fluid inlet temperature and surface earth temperature were analyzed.

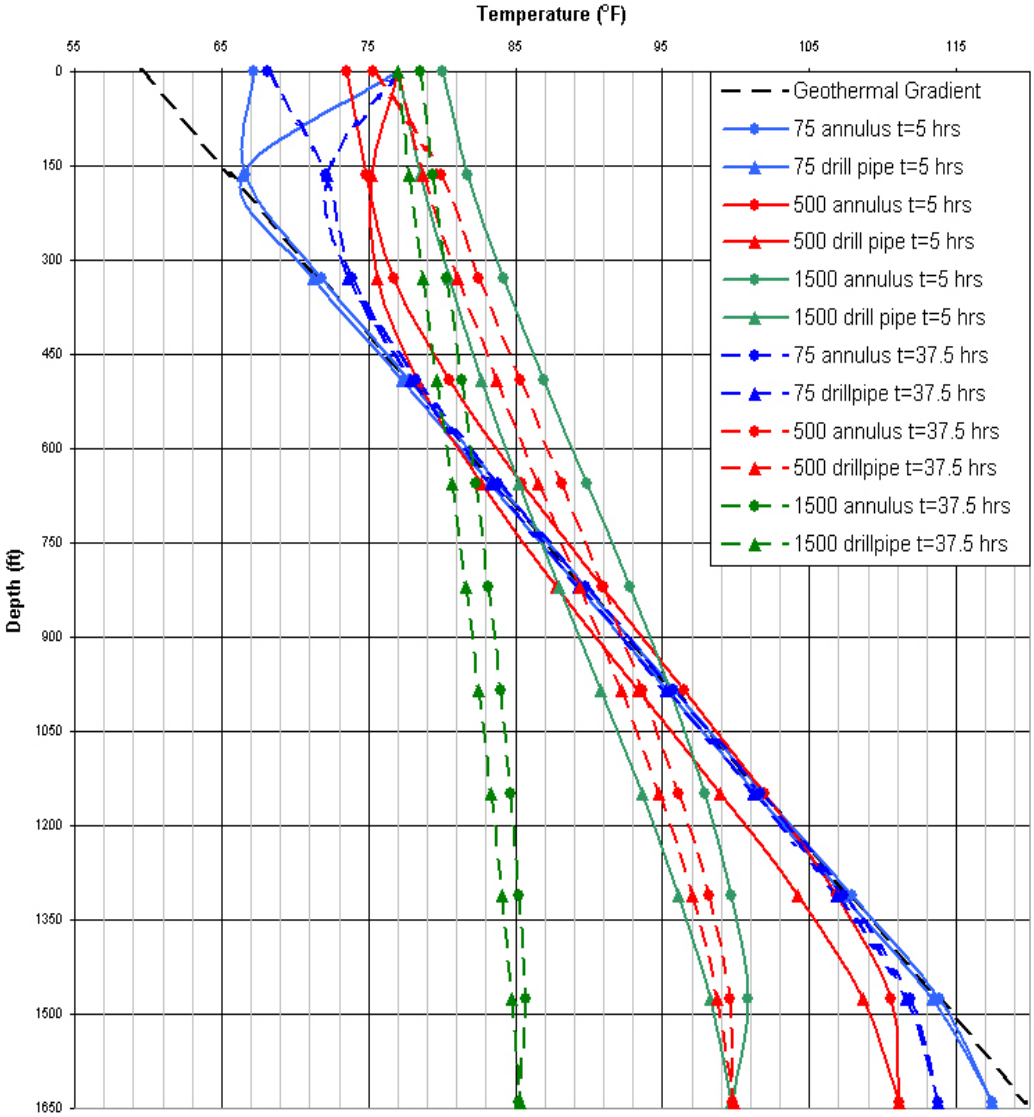

Figure 14. Change of temperature profile with different flow rates and time values at 1640 ft well.

Figure 14 demonstrates effect of time on different flow rates at a geothermal gradient of 3.65 ^{o}F/100ft. Low flow rates tended to be close to the geothermal gradient, thus were not significantly affected by time. As the flow rate increased, effects of time became more apparent. As it would be expected, a flow rate high as 1500 bbl/hr quickly cools the formation and approaches to a near vertical profile, that signifies little or no temperature change.

Change of temperature with respect to different formation conductivity values is presented in Figure 15. 6.85 ^{o}F/100ft geothermal gradient and 225 bbl/hr flow rate were was used in these simulations. As it can be seen in the figure, doubling or quadrupling the conductivity of the formation has an effect on the temperature on the order of 2-4°F, which is insignificant when compared to other variables.

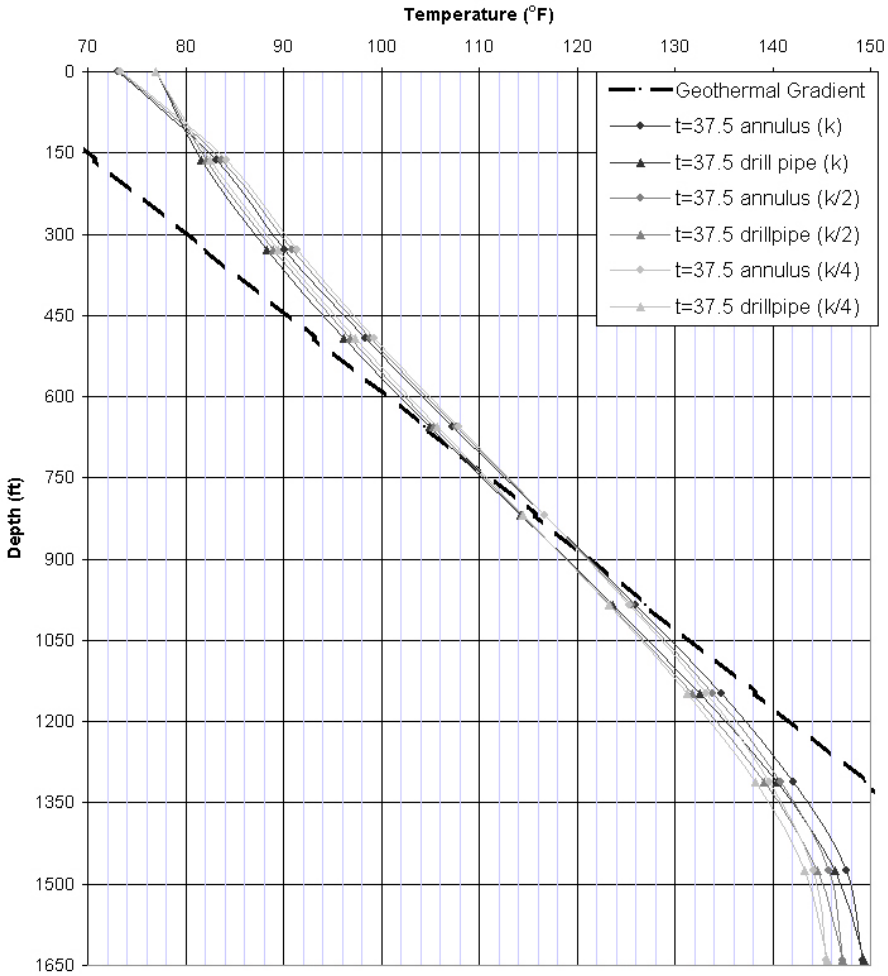

Figure 15. Change of temperature distribution with formation conductivity.

Notably, temperature of the annular fluid is less than inlet temperature. The reason for this is that the area annular fluid is exposed to the formation is larger than the area it is exposed to drill pipe, thus annular fluid loses heat energy to the formation more rapidly than it gets heat energy from the drill pipe. This is valid for all similar occurrences in this study.

Change of temperature with respect to different formation specific heat values is presented in Figure 16. 6.85 ^{o}F/100ft geothermal gradient and 225 bbl/hr flow rate were used in these simulations. Similarly to effect of formation conductivity, doubling or quadrupling the specific heat of the formation has an effect on the temperature on the order of 2-4°F, which is insignificant when compared to other variables.

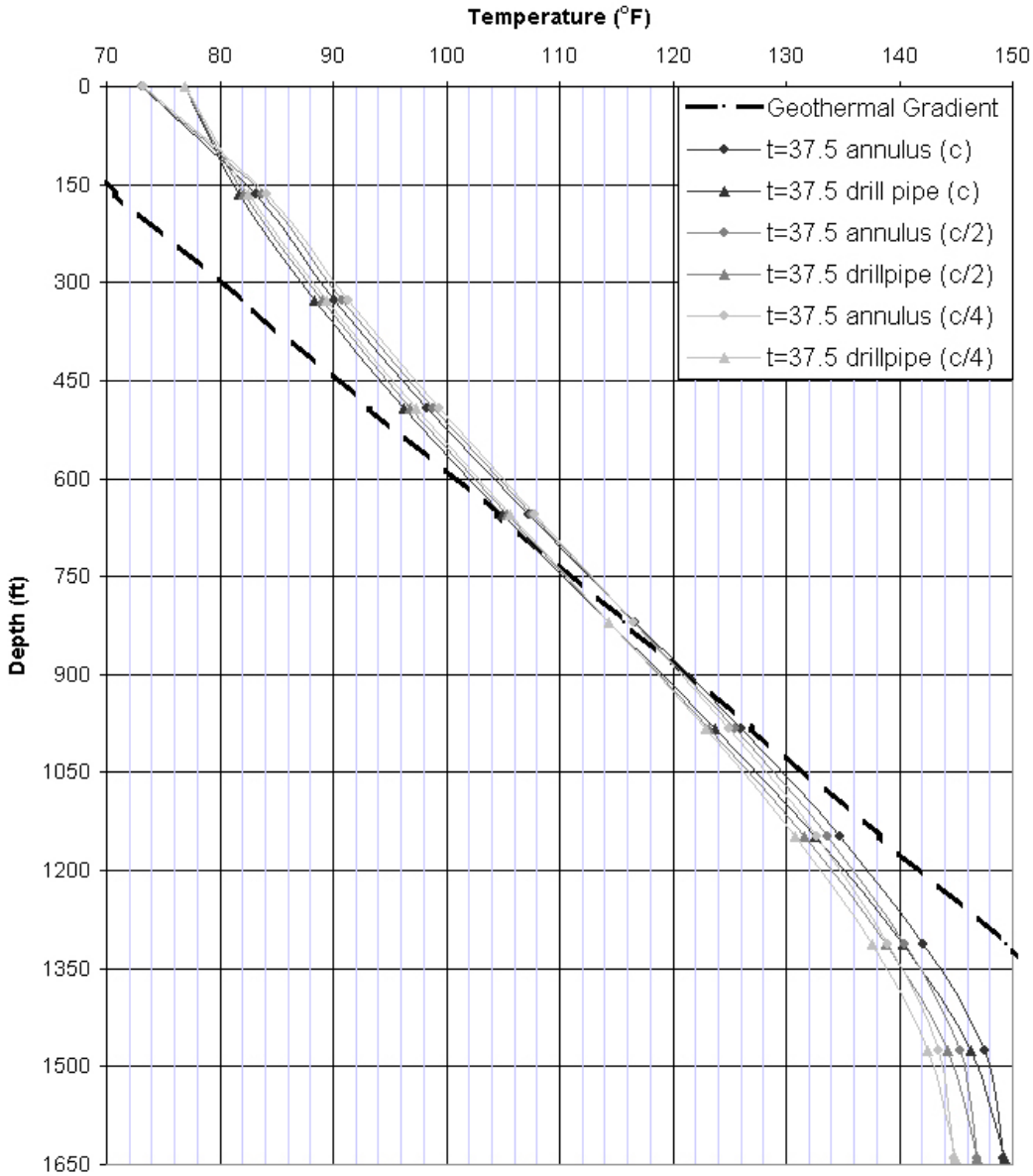

Figure 16. Change of temperature distribution with formation specific heat.

Change of temperature with respect to different fluid inlet temperature (T_{pi}) values is presented in Figure 17. 6.85 ^{o}F/100ft geothermal gradient and 500 bbl/hr flow rate were used in these simulations. The most significant effect of inlet temperature is on the overall temperature profile, however as it can be seen in the figure maximum temperature change occurs in the order of 3-4°F.

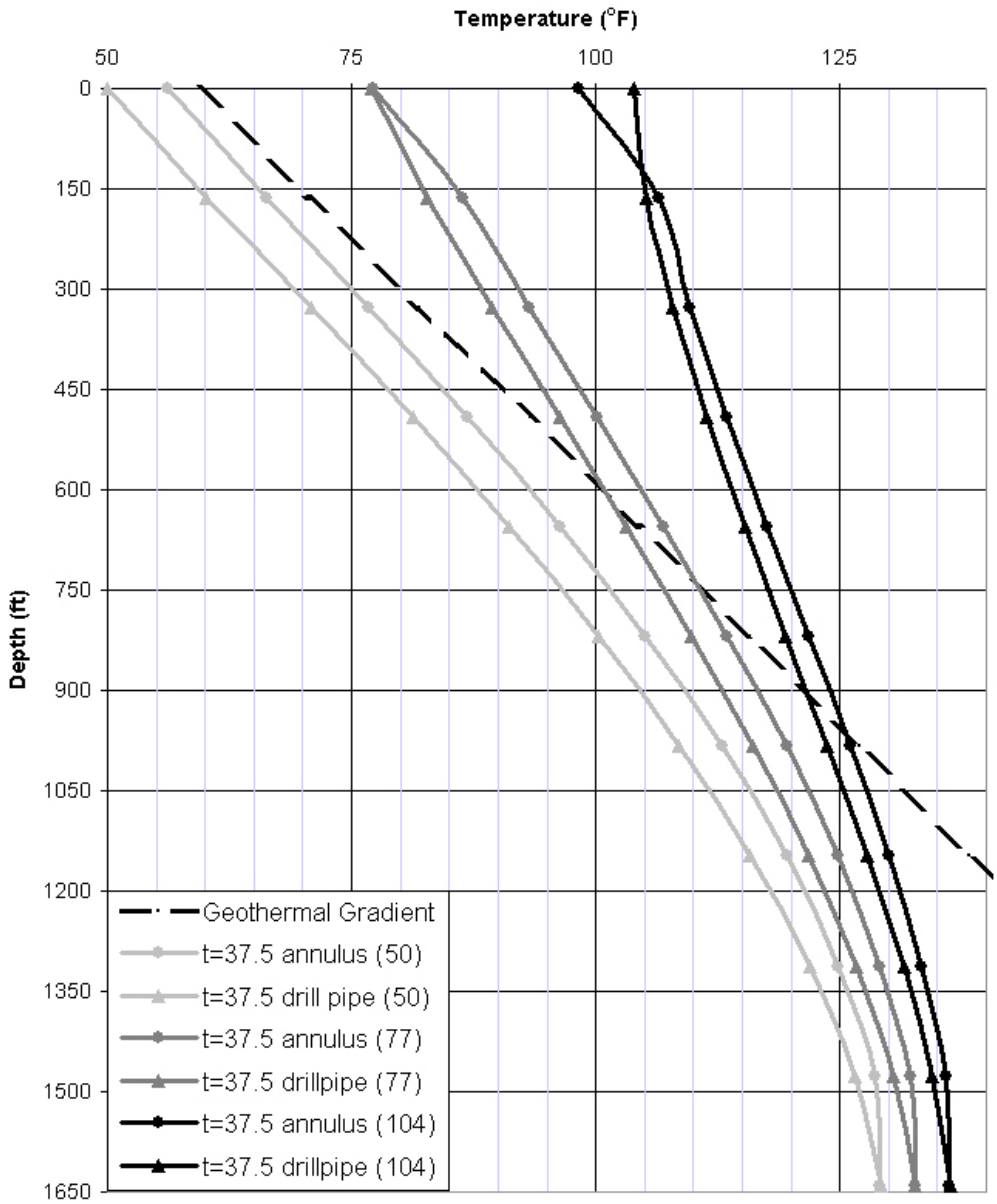

Figure 17. Change of temperature distribution with inlet fluid temperature (^{o}F).

Change of temperature with respect to different surface earth temperature (T_s) values is presented in Figure 18. 6.85 ^{o}F/100ft geothermal gradient and 500 bbl/hr flow rate were used in these simulations. Since this value shifts the temperature values at any given depth, maximum temperature of the fluid significantly changes.

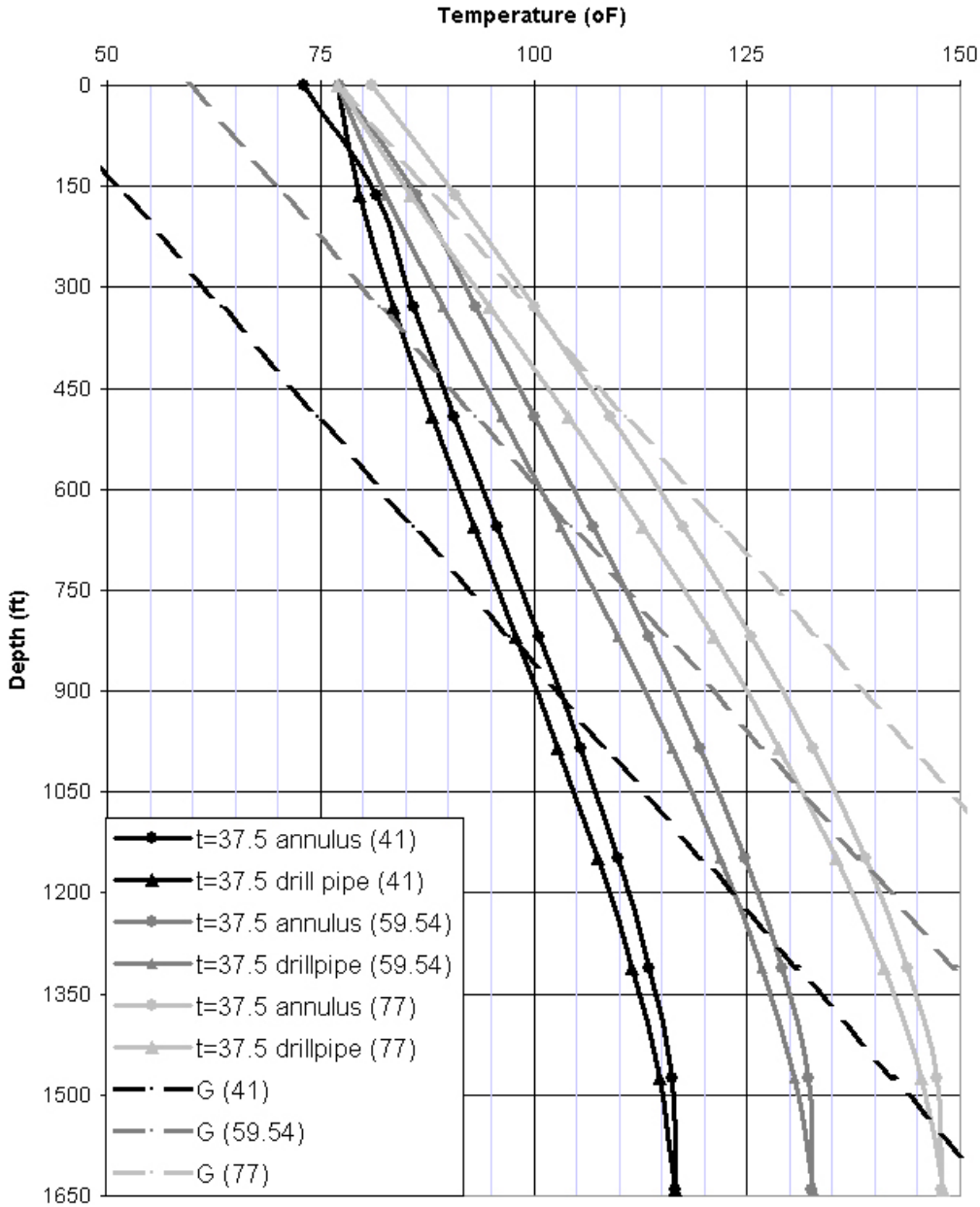

Figure 18. Change of temperature distribution with surface earth temperature (^{o}F).

Figure 19 demonstrates effect of time on different flow rates in the 3280 ft well, at a geothermal gradient of 3.65 ^{o}F/100ft. Similar to the 1640 ft well, low flow rates tended to stick to the geothermal gradient, nearly unaffected by time. High flow rates cool down the formation relatively quickly, and thus their corresponding temperature distribution lines approach a vertical profile of little or no temperature change. However, it can be observed from the green dashed lines depicting 1500 bbl/hr flow rate is farther away from that vertical profile than it was in the 1640 ft. well.

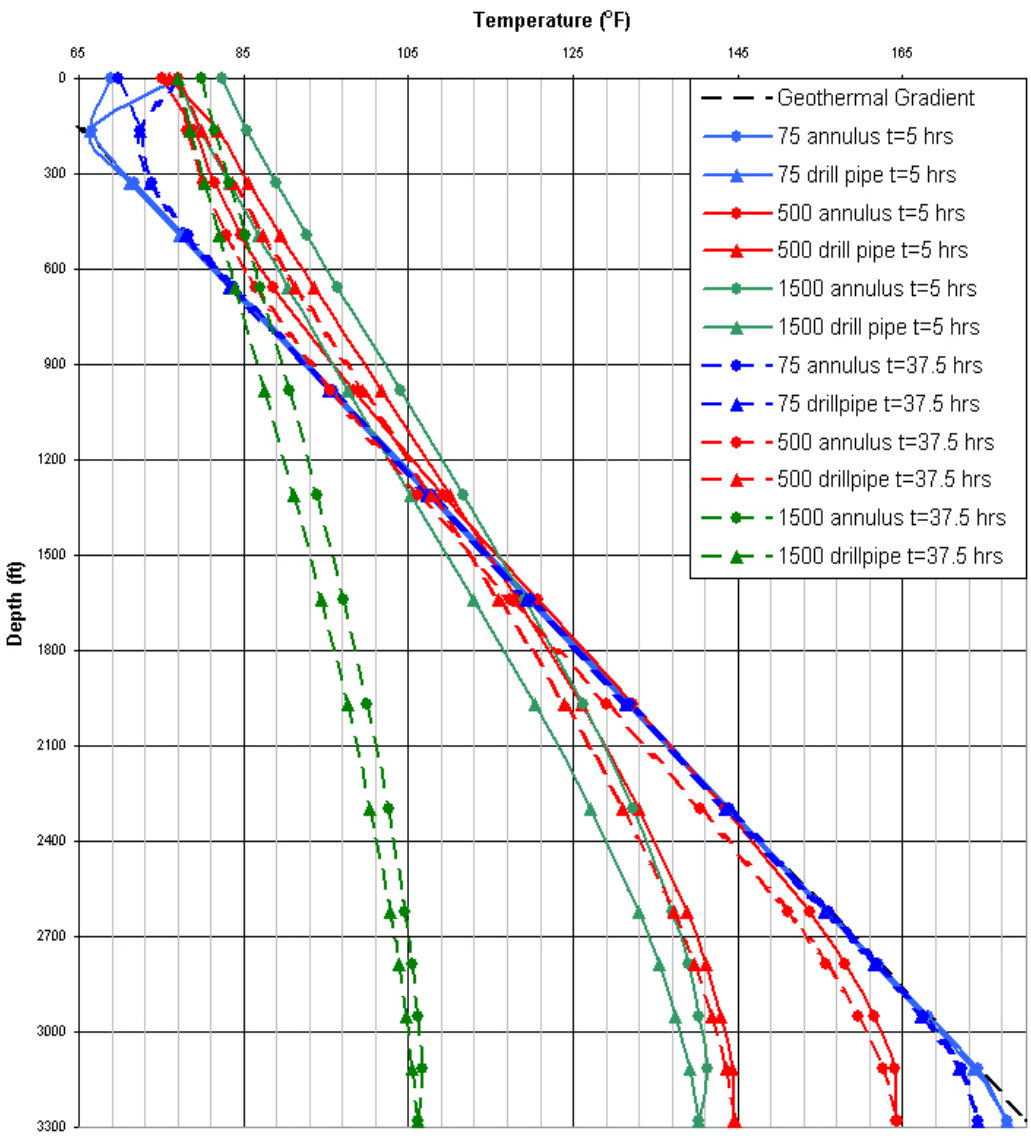

Figure 19. Change of temperature profile with different flow rates and time velues at 3280 ft well.

Figure 20 demonstrates effect of time on different flow rates in the 4920 ft well, at a geothermal gradient of 3.65 ^{o}F/100ft. Similar to the Figures 14 and 19, low flow rates appeared on the geothermal gradient. Higher flow rates showed some deviation, but due to increasing depth of the well these corresponding temperature distribution lines of these flow rates are far from the vertical no temperature change profile.

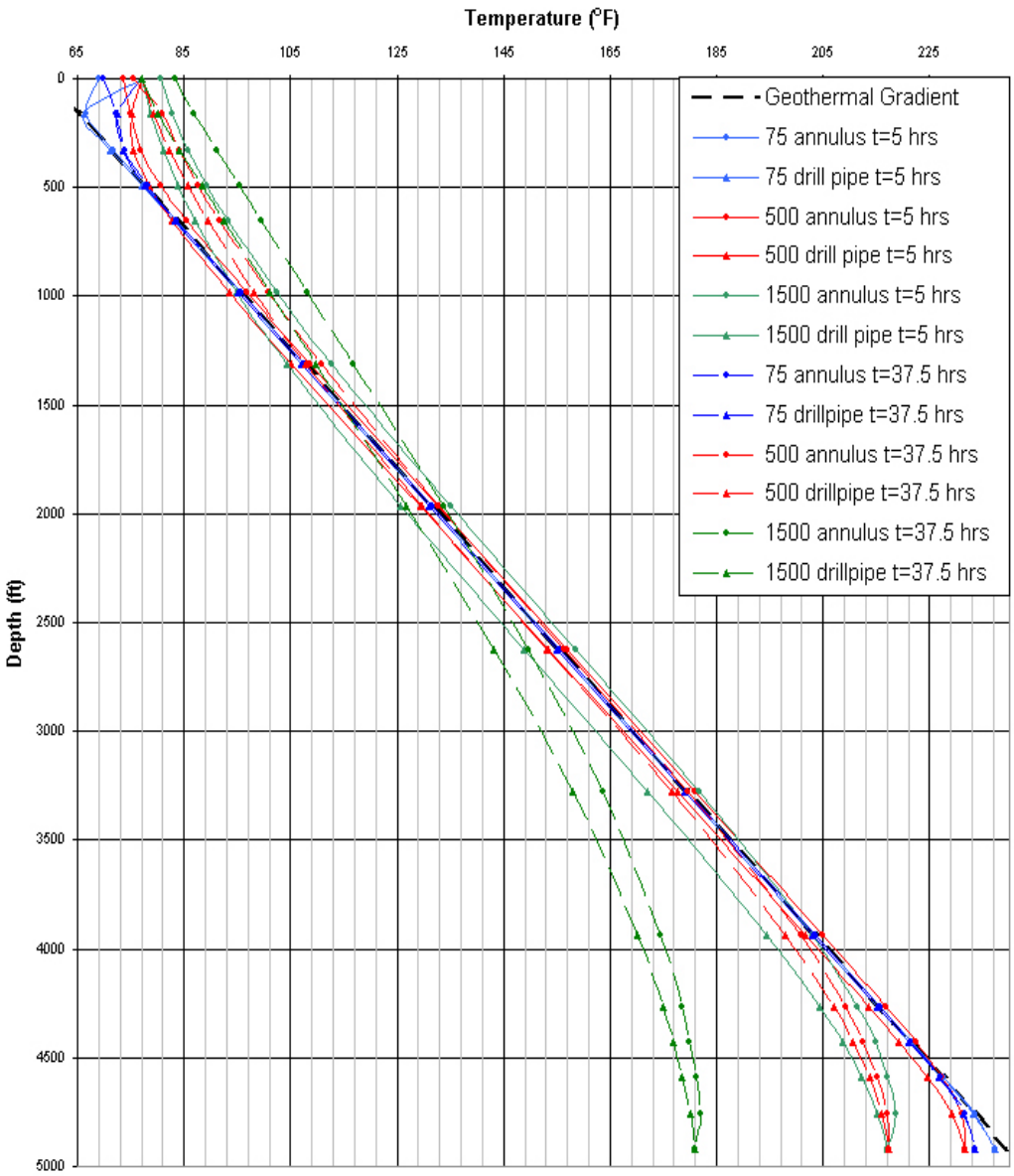

Figure 20. Change of temperature profile with different flow rates and time velues at 4920 ft well.

7.2.2. Correlation Results

As mentioned before, many different correlation methods were tried to derive equations for predicting temperature profile in both drill pipe and annulus. Correlation improvement was attempted by dimensional analysis. Simplest of the equations yielded the most accurate results. Figure 21 demonstrates the simulation data and corresponding calculated data. Results were obtained for 37.5 hr at a geothermal gradient of 6.85 ^{o}F/100ft.

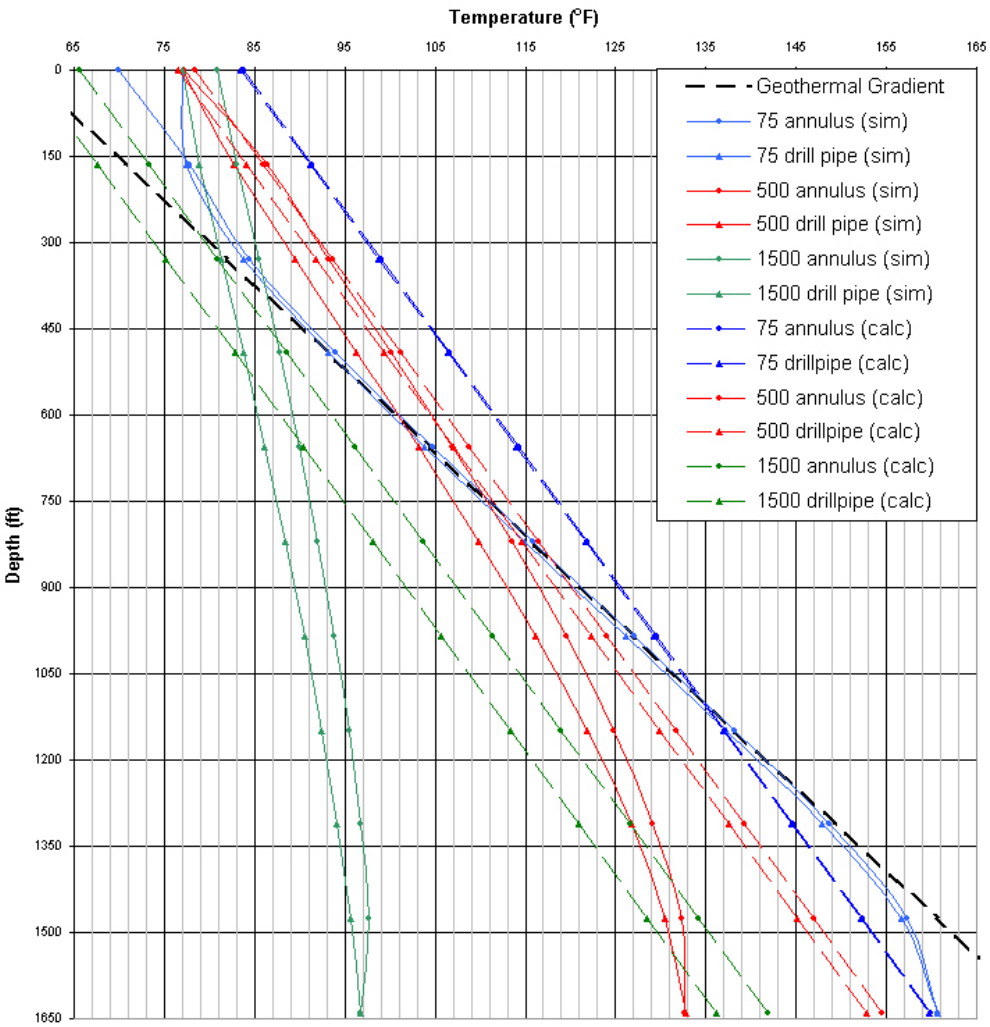

Figure 21. Correlation results with simulation data.

Linear correlation generally worked well for moderate flow rates, but it lacked the accuracy to estimate behavior of high flow rates.

The plot of simulated well data and data calculated from the linear correlation for annulus (equation 2) is presented in Figure 21.

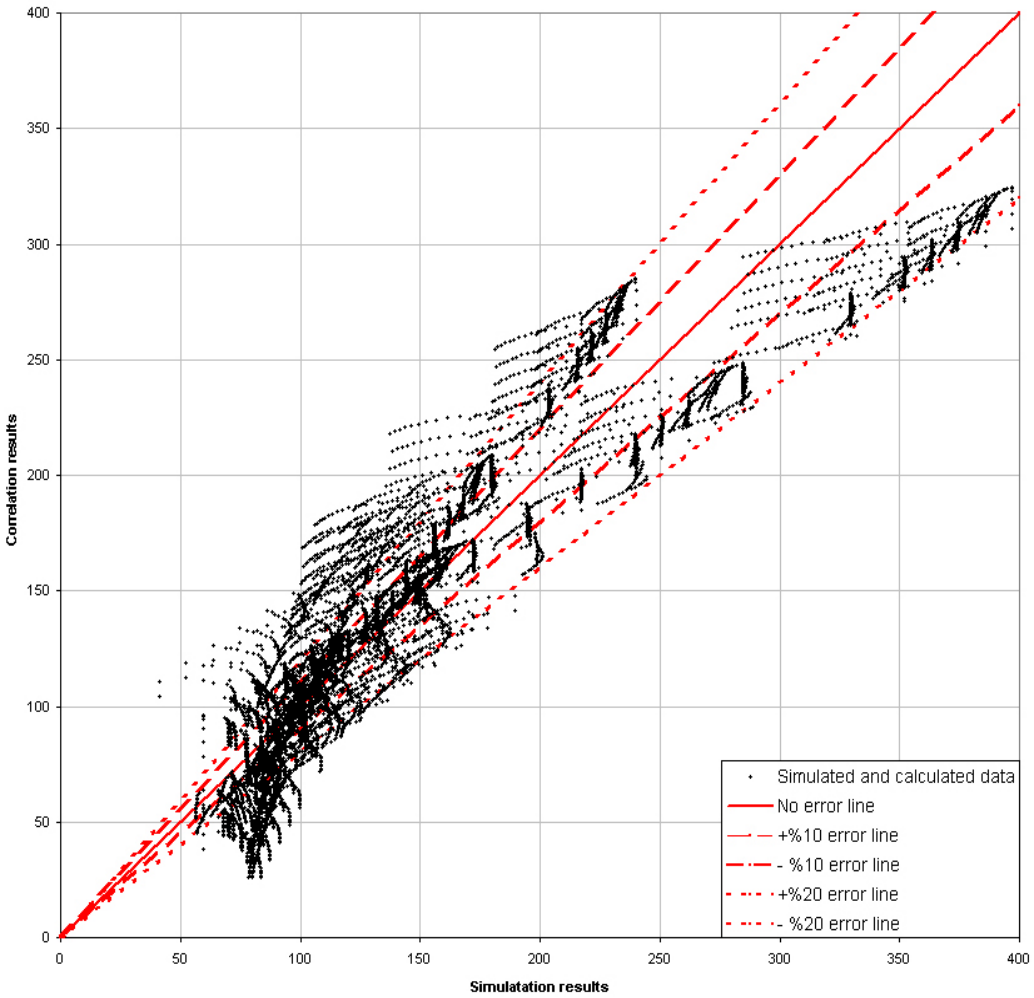

Figure 22. Accuracy of temperature approximation in the annulus.

Results from the computer simulation are on x-axis and correlation results are on the y-axis. Solid red line represents the perfect match; coarsely dashed lines represent ±%10 deviation and finely dashed lines represent ±%20 deviation from the match. The average error is less than %16. Low and high temperature estimation errors are especially high, because correlation is linear, thus does not approximate the deviations of the temperature at near surface and bottom-hole zones.

The plot of simulated well data and data calculated from the linear correlation for drillpipe (equation 1) is presented in Figure 23.

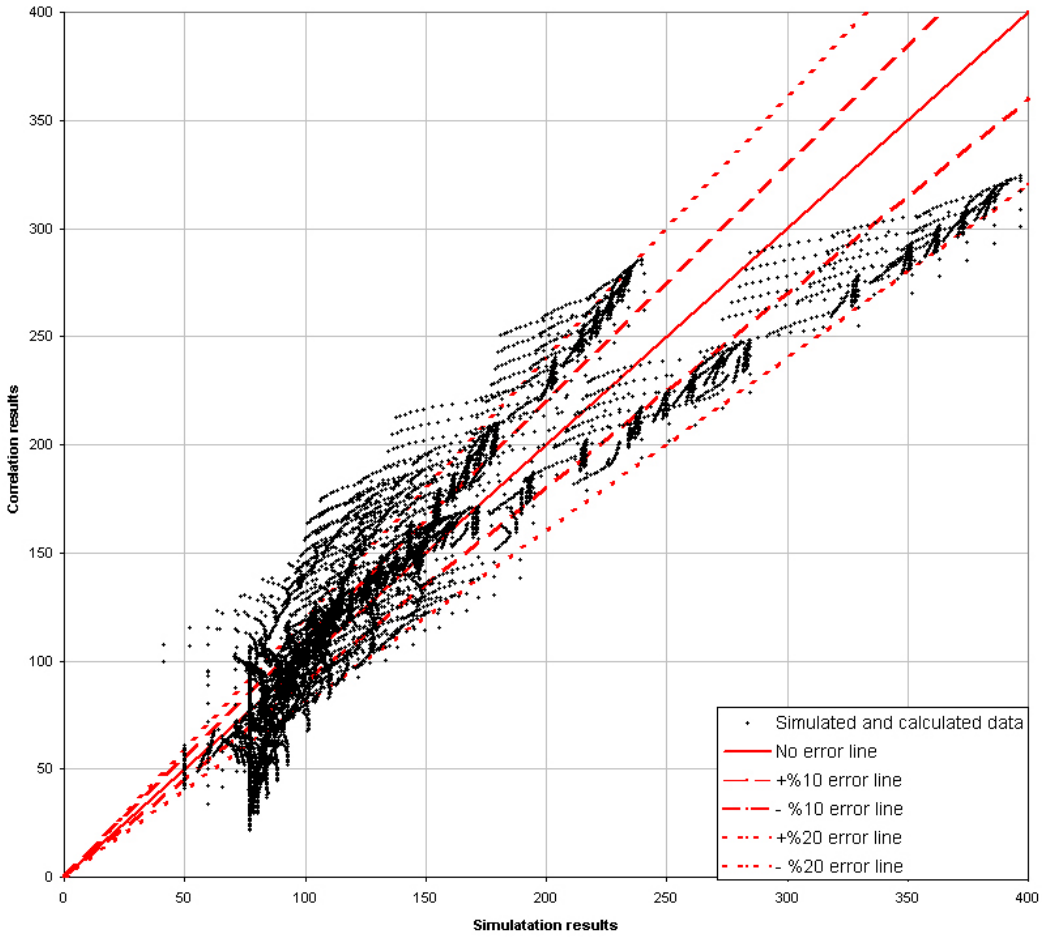

Figure 23. Accuracy of temperature approximation in the drill pipe.

Results from the computer simulation are on x-axis and correlation results are on the y-axis. Solid red line represents the perfect match; coarsely dashed lines represent ±%10 deviation and finely dashed lines represent ±%20 deviation from the match. The average error is less than %16. Similar to annulus correlation, low and high temperature estimation errors are especially high, because correlation is linear, thus does not approximate the deviations of the temperature at near surface and bottom-hole zones.

Matching both temperature profile data and simulated data was not essential, since the main objective was to obtain an expression for the maximum temperature in the wellbore. Figure 24 demonstrates the accuracy of the linear maximum temperature estimation (Equation 3).

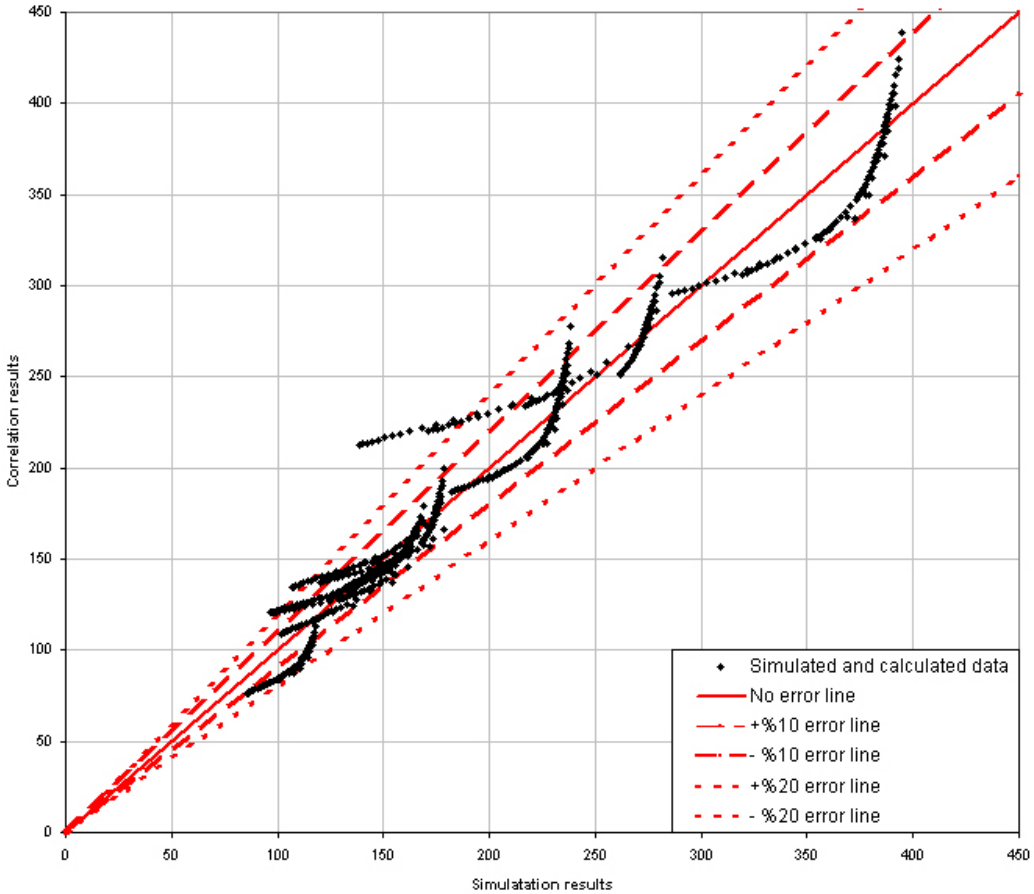

Figure 24. Accuracy of maximum temperature estimation.

Results from the computer simulation are on x-axis and correlation results are on the y-axis. Solid red line represents the perfect match; coarsely dashed lines represent ±%10 deviation and finely dashed lines represent ±%20 deviation from the match. The average error is less than %7, which is acceptable in field operations. Individual points rarely gets outside the ±%20 deviation lines.

7.3. Comparison

Since analytical solution produces no accurate results for the depths the simulations were run, direct comparison was not possible. However, Holmes and Swift [10] model, which is given in Appendix A, still provided nearly tangible data. Comparison of simulation and calculated data is given in Figure 25. Wellbore geometry was adapted from the computer model, geothermal gradient was 6.85 ^{o}F/100ft and depth was set at 3280 ft.

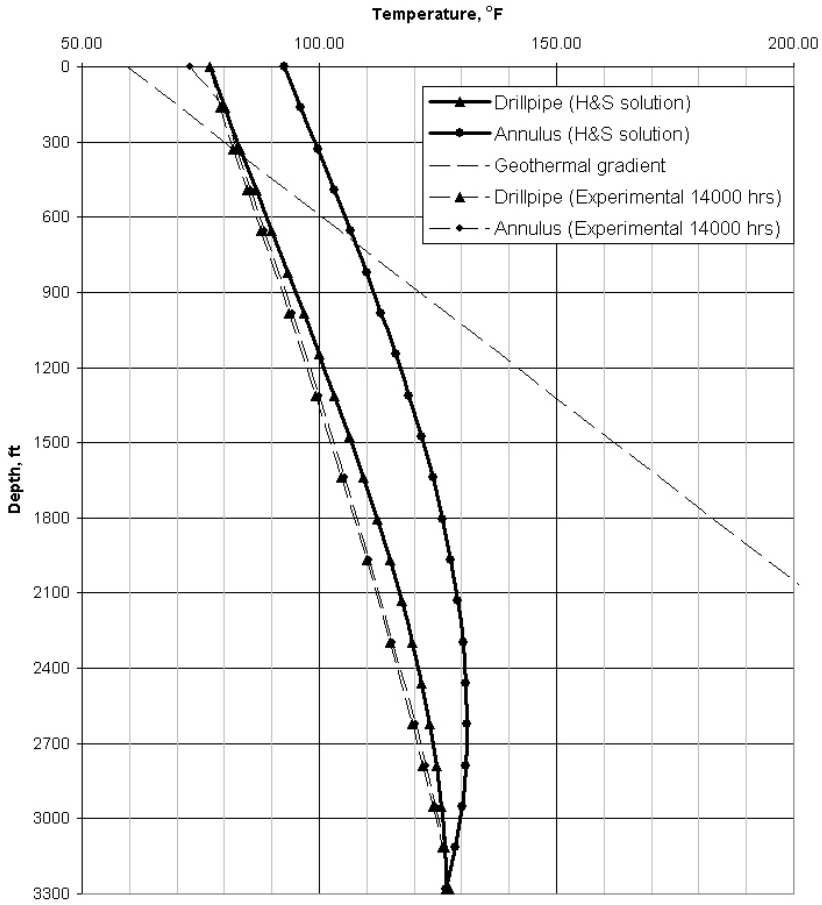

Figure 25. Simulation and analytically calculated data comparison.

Black lines representing the Holmes and Swift [9] steady state solution, unlike the red lines representing the computer simulation data, are far too apart from each other, and thus fails to predict cool-down of the formation.

CHAPTER 8

CONCLUSION

Temperature profile in a circulating well is analyzed. An analytical model with its results for a number of different scenarios is presented. The model is applied for a well with casing strings and changes to the temperature profile are observed. A computer program is written for easy implementation. It has been observed that below 12000 ft the analytical solution starts to give unreliable results. In the second part of the study, a computer program is used to simulate a circulating well. Similar scenarios are analyzed with this program and results are recorded. Finally, empirical correlations are sought in this data to obtain a simpler model for predicting maximum circulating fluid temperature. The results are analyzed and compared with other studies, hence following conclusions are drawn:

- Analytical models, one of which is presented in this study are only reliable in deep wells.

- Temperature profile in a circulating well is strongly dependent on circulation rate and circulation time. As the circulation rate increases, the profile tends to show a cool down effect and as the circulation time increase, formation cools down and, thus, heat transfer from the

formation decreases, which also shows itself as a general temperature drop in circulating fluid.

- It has been observed that inlet temperature of the drilling fluid has little or no impact on the maximum drilling fluid temperature in a well.

- Addition of possible casing strings to the model has very little effect on the final result. The temperature profile curves are affected but maximum drilling fluid temperature shows no significant change.

- Thermal properties of the formation, namely specific heat and conductivity with their window of change, don't have a significant effect on maximum drilling fluid temperature in a flowing well.

- Approximation derived for temperature profiles in annulus and wellbore is accurate enough to give an idea with an average error of %15.5.

- Maximum temperature estimation is accurate enough to be used in the field with an average error of %6.7.

REFERENCES

[1] Srini-Vasan, S., Gatlin, C., "The Effect of Temperature on the Flow Properties of Clay-Water Drilling Muds", Jour. Pet. Tech (December, 1958).

[2] Hiller, K.H., "Rheological Measurements on Clay Suspensions and Drilling Fluids at High Temperatures and Pressures", Jour. Pet. Tech. (July, 1963) 779.

[3] Weintritt, D.J., Hughes, R.G. Jr., "Factors Involved in High-Temperature Drilling Fluids", Jour. Pet. Tech. (June, 1965) 707-716.

[4] Annis, M.R., "High-Temperature Flow Properties of Water-Base Drilling Fluids", Jour. Pet. Tech. (1967) 1074.

[5] Chesser, B.G., Enright, D.P., "High-Temperature Stabilization of Drilling Fluids With a Low-Molecular-Wight Copolymer", Jour. Pet. Tech. (1980) 950.

[6] Amanullah, Md., "An Environment Friendly and Economically Attractive Thermal Degradation Inhibitor for Bentonite Mud", SPE Europec/EAGE Annual Conference and Exhibition, Vienna, Austria (June 12-15, 2006).

[7] Browning, W.C., Perrieone, A.C., "Clay Chemistry and Drilling Fluids", paper SPE 540 presented at SPE First Conference on Drilling and Rock Mechanics, The U. of Texas, Austin (January 23-24, 1963).

[8] Butts, H.B., Hise, B.R., "The Effect of Temperature on Pressure Losses During Drilling", Jour. Pet. Tech. (1973).

[9] Ramey, H.J. Jr., "Wellbore Heat Transmission", Jour. Pet. Tech. (April 1962) 427.

[10] Holmes, C.S., Swift, S.C., "Calculation of Circulating Mud Temperatures", Jour. Pet. Tech (1969).

[11] Raymond, L.R., “Temperature Distribution in a Circulating Drilling Fluid”, Jour. Pet. Tech (1969).

[12] Keller, H.H., Couch, E.J., Berry, P.M., “Temperature Distribution in Circulating Mud Columns”, Jour. Pet. Tech (February, 1973).

[13] Tansev, E., Startzman, R.A., Cooper, A.M., “Predicting Pressure Loss and Heat Transfer in Geothermal Wellbores”, Jour. Pet. Tech (1975).

[14] Thompson, M., Burgess, T.M., “The Prediction of Interpretation of Mud Temperature While Drilling”, Jour. Pet. Tech (September, 1985).

[15] Bittleston, S.H., “A Two-Dimensional Simulator To Predict Circulating Temperatures During Cementing Operations”, Jour. Pet. Tech (September, 1990).

[16] Alves, I.N., Alhanatl, F.J.S., Shoham, O., “A Unified Model for Predicting Flowing Temperature Distribution in Wellbores and Pipelines”, Jour. Pet. Tech (November, 1992).

[17] Kabir, C.S., Hasan, A.R., Kouba, G.E., Ameen, M.M., “Determining Circulating Fluid Temperature in Drilling, Workover, and Well Control Operations”, Jour. Pet. Tech (January, 1996) 74-79.

[18] Hasan, A.R., Kabir, C.S., Ameen, M.M., “A Mechanistic Model for Circulating Fluid Temperature”, Jour. Pet. Tech (June, 1996) 135-143.

[19] Karstad, E., Aadney, B.S., “Optimization of Mud Temperature and Fluid Models in Offshore Applications”, Jour. Pet. Tech (September, 1999).

[20] Hagoort, J., “Ramey's Wellbore Heat Transmission Revisited”, SPE Journal (December, 2004) 465-474.

[21] McAdams, W.H., ”Heat Transmission”, Third Ed., McGraw-Hill Book Co., Inc., N.Y. (1954).

[22] Hasan, A.R., Kabir, C.S., “Aspects of Wellbore Heat Transfer During Two-Phase Flow”, SPE Production and Facilities (August, 1994).

APPENDIX A

Holmes and Swift's Steady State Model

This model is important because it is simple and widely in use. It has similar assumptions, except the steady state heat transfer from the formation. The same heat balance is made on the differential element in figure 26.

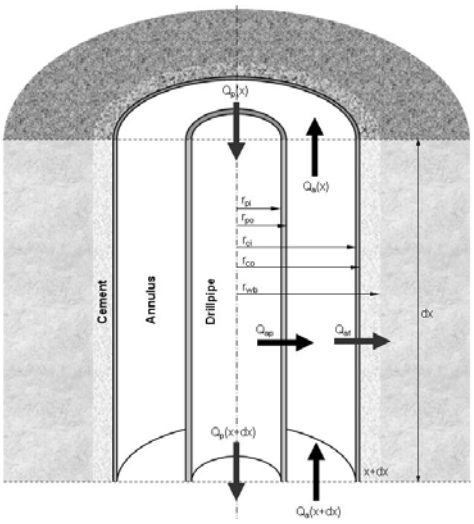

Figure 26. Diagram of the wellbore that has a length of dx (Used in Holmes & Swift [10] Model).

$$\dot{Q}_a(x) - \dot{Q}_a(x+dx) + \dot{Q}_{ap} = \dot{Q}_{af} \tag{A.1}$$

$$\dot{Q}_a(x) - \dot{Q}_a(x+dx) = mc_p\left(T_{ax} - T_{a(x+dx)}\right) \tag{A.2}$$

$$\dot{Q}_{ap} = 2\pi r_{pi} U_p (T_p - T_a) dx \tag{A.3}$$

For the approximation of formation heat flux, following equation is used,

$$\dot{Q}_{af} = 2\pi r_{ci} U_a (T_a - T_f) dx \tag{A.4}$$

The heat balance on the annular element, equation (A.1) becomes,

$$mc_p \left(T_{ax} - T_{a(x+dx)}\right) + 2\pi r_{pi} U_p (T_p - T_a) dx = 2\pi r_{ci} U_a (T_a - T_f) dx \tag{A.5}$$

$$mc_p \frac{dT_a}{dx} + 2\pi r_{pi} U_p (T_p - T_a) = 2\pi r_{ci} U_a \left(T_a - T_s - Gx\right) \tag{A.6}$$

A similar development would give the heat balance for the drill stem,

$$mc_p \frac{dT_p}{dx} = 2\pi r_{pi} U_p (T_p - T_a) \tag{A.7}$$

The differential equations are similarly solved as given in the chapter 5. The resulting solutions are as follows,

$$T_a = K_1 e^{C_1 x} + K_2 e^{C_2 x} + Gx + T_s - GA \tag{A.8}$$

$$T_p = K_1 C_3 e^{C_1 x} + K_2 C_4 e^{C_2 x} + Gx + T_s \tag{A.9}$$

Where,

$$C_1 = \frac{B}{2A}\left[1 + \sqrt{1 + \frac{4}{B}}\right] \qquad C_2 = \frac{B}{2A}\left[1 - \sqrt{1 + \frac{4}{B}}\right]$$

$$C_3 = 1 + \frac{B}{2}\left[1 + \sqrt{1 + \frac{4}{B}}\right] \qquad C_4 = 1 + \frac{B}{2}\left[1 - \sqrt{1 + \frac{4}{B}}\right]$$

$$A = \frac{mc_p}{2\pi r_{pi} U_p} \qquad B = \frac{r_{ci} U_a}{r_{pi} U_p}$$

$$K_1 = T_{pi} - K_2 - T_s + GA \qquad K_2 = \frac{GA - \left(T_{pi} - T_s + GA\right) e^{C_1 H} \left(1 - C_3\right)}{e^{C_2 H} \left(1 - C_4\right) - e^{C_1 H} \left(1 - C_3\right)}$$

APPENDIX B

Sample Calculation for Openhole Well

This sample is calculated for a circulation time of 44 hours and depth of 12000 ft. Well and drilling fluid data from Holmes and Swift [10] is used as given below,

Table 1. Well and drilling fluid data from Holmes and Swift [10]

Well Depth, ft	15000
Drill Stem OD, in	6.625
Drill Bit size, in	8.375
Circulation Rate, bbl/hour	300
Inlet Drilling fluid Temperature, ^{o}F	60
Drilling fluid Viscosity, lb/(ft-hr)	110
Drilling fluid Thermal Conductivity, Btu/(ft-^{o}F-hr)	1
Drilling fluid Specific Heat, Btu/(lb-^{o}F)	0.4
Drilling fluid Density, lb/gal	10
Formation Thermal Conductivity, Btu/(ft-^{o}F-hr)	1.3
Formation Specific Heat, Btu/(lb-^{o}F)	0.2
Formation Density, Lb/ft^3	165
Surface Earth Temperature, ^{o}F	59.5
Geothermal Gradient, ^{o}F/ft	0.0127

N_{RE} values for both drillpipe and annulus and N_{Pr} are calculated,

$$N_{REp} = \frac{2r_{pi}m}{A_p\mu} = \frac{(2)(6.375\text{ in})(300\text{ B/hr})}{\pi(6.375\text{ in})^2(110\text{ lb/ft-hr})}(2)(12\text{ in/ft})(10\text{ lb/gal})(42\text{ gal/B})$$

$$N_{REp} = 2746.7$$

$$N_{REa} = 0.816\frac{2\left(r_{wb} - r_{po}\right)m}{A_a\mu}$$

$$= \frac{(0.816)(2)(8.375 \text{ in - } 6.625 \text{ in})(300 \text{ B/hr})}{\pi\left[(8.375 \text{ in})^2 \text{ - } (6.625 \text{ in})^2\right](110 \text{ lb/ft-hr})}(2)(12 \text{ in/ft})(10 \text{ lb/gal})(42 \text{ gal/B})$$

$$N_{REa} = 952.6$$

$$N_{\Pr} = \frac{c_p}{\mu k} = \frac{(0.4 \text{ Btu/lb-}^0\text{F})}{(110 \text{ lb/ft-hr})(1 \text{ Btu/ft-lb-}^0\text{F})} = 44.00$$

Coefficients of heat transfer of drilling fluid in drillpipe and annulus are,

$$h_p = 0.023\left[N_{RE}\right]^{0.8}\left[N_{\Pr}\right]^{0.4}\frac{k}{2r_{pi}} = (0.023)(2746.7)^{0.8}(44)^{0.4}\frac{(12 \text{ in/ft})(2)(1 \text{ Btu/ft-lb-}^0\text{F})}{(6.375 \text{ in})}$$

$$h_p = 110.88 \text{ Btu/hr-sq ft-}^{\text{o}}\text{F}$$

$$h_a = 0.023\left[N_{RE}\right]^{0.8}\left[N_{\Pr}\right]^{0.4}\frac{k}{2r_{wb}} = (0.023)(952.6)^{0.8}(44)^{0.4}\frac{(12 \text{ in/ft})(2)(1 \text{ Btu/ft-lb-}^0\text{F})}{(8.375 \text{ in})}$$

$$h_a = 36.18 \text{ Btu/hr-sq ft-}^{\text{o}}\text{F}$$

Overall heat transfer coefficients are calculated by using following equations,

$$\frac{1}{U_p} = \frac{1}{(110.88 \text{ Btu/hr-sq ft-}^0\text{F})} + \frac{(6.375 \text{ in})}{(600\text{Btu/ft-lb-}^0\text{F})(2)(12 \text{ in/ft})}Ln\left(\frac{6.625 \text{ in}}{6.375 \text{ in}}\right)$$

$$+\frac{(6.375 \text{ in})}{(6.625 \text{ in})}\frac{1}{(36.18 \text{ Btu/hr-sq ft-}^0\text{F})}$$

$U_p = 28.06$ Btu/hr-sq ft-^{o}F

$$\frac{1}{U_a} = \frac{1}{h_a} = \frac{1}{\left(36.18 \text{ Btu/hr-sq ft-}^0\text{F}\right)}$$

$U_a =$ 36.18 Btu/hr-sq ft-^{o}F

Dimensionless temperature function is,

$$\alpha = \frac{k_f}{c_f \rho_f} = \frac{\left(1.3 \text{ Btu/(ft-}^o\text{F-hr)}\right)}{\left(0.2 \text{ Btu/(lb-}^o\text{F)}\right)\left(165 \text{ lb/ft3}\right)} = 0.039 \text{ sq ft/hr}$$

$$t_D = \frac{\alpha t}{r_{wb}^2} = \frac{\left(0.039 \text{ sq ft/hr}\right)\left(44 \text{ hr}\right)}{\left[\frac{\left(8.375 \text{ in}\right)}{\left(2\right)\left(12 \text{ in/ft}\right)}\right]^2} = 14.2 \quad > 1.5$$

$$T_D = \left[0.4063 + 0.5\ln\left(14.2\right)\right] \times \left(1 + \frac{0.6}{\left(14.2\right)}\right) = 1.81$$

Derivation constants are,

$$A = \frac{2\pi r_{pi} U_p}{mc_p} = \frac{\pi\left(2\right)\left(6.375 \text{ in}\right)\left(28.06 \text{ Btu/hr-sq ft-oF}\right)}{\left(2\right)\left(12 \text{ in/ft}\right)\left(300 \text{ B/hr}\right)\left(10 \text{ lb/gal}\right)\left(42 \text{ gal/B}\right)\left(600\text{Btu/ft-lb-}^0\text{F}\right)}$$

$A = 0.000929$

$$B = \frac{2\pi r_{ci} U_a k_f}{mc_p\left(k_f + r_{ci} U_a T_D\right)} = \frac{\pi\left(2\right)\left(8.625 \text{ in}\right)\left(36.18 \text{ Btu/hr-sq ft-oF}\right)\left(1.3 \text{ Btu/(ft-}^o\text{F-hr)}\right)}{\left(2\right)\left(12 \text{ in/ft}\right)\left(300 \text{ B/hr}\right)\left(10 \text{ lb/gal}\right)\left(42 \text{ gal/B}\right)\left(600\text{Btu/ft-lb-}^0\text{F}\right)} \frac{1}{\left[\left(1.3 \text{ Btu/(ft-}^o\text{F-hr)}\right) + \frac{\left(8.625 \text{ in}\right)}{\left(2\right)\left(12 \text{ in/ft}\right)}\left(36.18 \text{ Btu/hr-sq ft-oF}\right)\left(1.81\right)\right]}$$

$B =$ 0.0000848

$$\theta_1 = \frac{B + \sqrt{B^2 + 4AB}}{2} = 0.000326$$

$$\theta_2 = \frac{B - \sqrt{B^2 + 4AB}}{2} = \text{-0.000241}$$

$$C_1 = \frac{\left(T_{pi} - T_s + \frac{G}{A}\right)\theta_2 e^{\theta_2 H} - G}{\left(\theta_1 e^{\theta_1 H} - \theta_2 e^{\theta_2 H}\right)} = \text{-0.296}$$

$$C_2 = \frac{\left(T_{pi} - T_s + \frac{G}{A}\right)\theta_1 e^{\theta_1 H} - G}{\left(\theta_1 e^{\theta_1 H} - \theta_2 e^{\theta_2 H}\right)} = 28.878$$

Applying the final equations to obtain temperature in drillpipe and annulus yields,

$$T_p = C_1 e^{\theta_1 x} + C_2 e^{\theta_2 x} + Gx + T_s - \frac{G}{A}$$

$$T_p = (-0.296)e^{(0.000326)(12000\text{ ft})} + (28.878)e^{(-0.000241)(12000\text{ ft})}$$
$$+ (0.0127\ ^{\circ}\text{F/ft})(12000\text{ ft}) + (59.5\ ^{\circ}\text{F}) - \frac{(0.0127\ ^{\circ}\text{F/ft})}{(0.000929)}$$

$$T_p = \mathbf{184.97\ ^{o}F}$$

$$T_a = \left(1 + \frac{\theta_1}{A}\right)C_1 e^{\theta_1 x} + \left(1 + \frac{\theta_2}{A}\right)C_2 e^{\theta_2 x} + Gx + T_s$$

$$T_a = \left(1 - \frac{(0.296)}{(0.000929)}\right)e^{(0.000326)(12000\text{ ft})} + \left(1 + \frac{(28.878)}{(0.000929)}\right)e^{(-0.000241)(12000\text{ ft})}$$
$$+ (0.0127\ ^{\circ}\text{F/ft})(12000\text{ ft}) + (59.5\ ^{\circ}\text{F})$$

$$T_a = \mathbf{193.02\ ^{o}F}$$

APPENDIX C

Sample Calculation for a Well with Three Casing Strings

This calculation is also based on Holmes and Swift [10] drilling fluid and well data. Additionally, there are three casing strings as shown in figure 27.

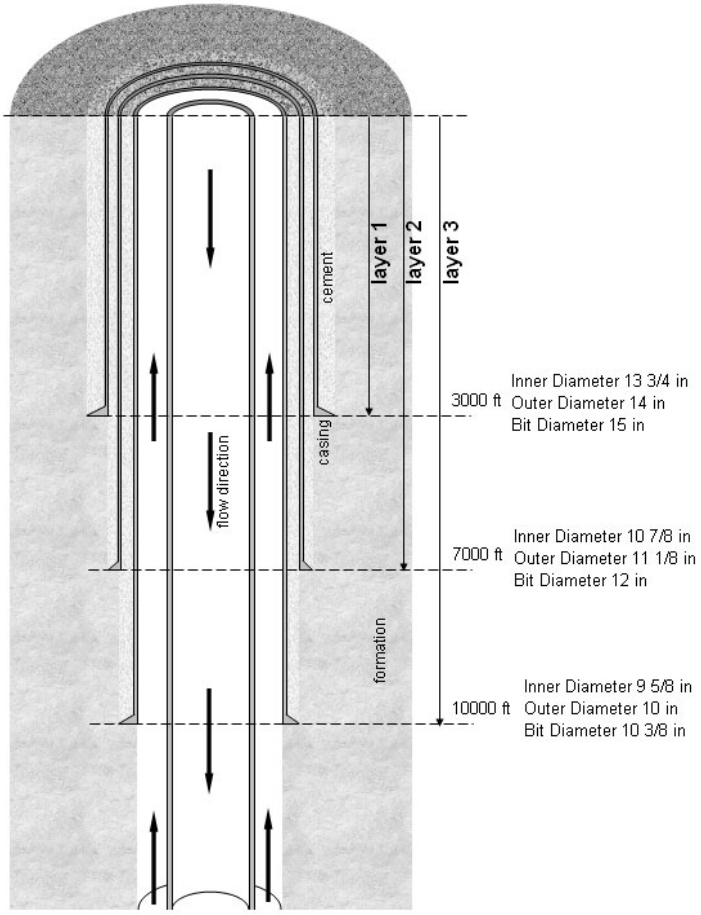

Figure 27. Casing strings used in sample calculation

This sample is calculated for a circulation time of 44 hours and depth of 2500 ft. Well and drilling fluid data from Holmes and Swift [10] is used as given in table 1. N_{RE} values for both drillpipe and annulus and N_{Pr} are calculated,

$$N_{REp} = \frac{2r_{pi}m}{A_p\mu} = \frac{(2)(6.375\text{ in})(300\text{ B/hr})}{\pi(6.375\text{ in})^2(110\text{ lb/ft-hr})}(2)(12\text{ in/ft})(10\text{ lb/gal})(42\text{ gal/B})$$

$$N_{REp} = 2746.7$$

$$N_{REa} = 0.816\frac{2(r_{wb} - r_{po})m}{A_a\mu}$$

$$= \frac{(0.816)(2)(9.625\text{ in - }6.625\text{ in})(300\text{ B/hr})}{\pi\left[(9.625\text{ in})^2 - (6.625\text{ in})^2\right](110\text{ lb/ft-hr})}(2)(12\text{ in/ft})(10\text{ lb/gal})(42\text{ gal/B})$$

$$N_{REa} = 879.28$$

$$N_{\Pr} = \frac{c_p}{\mu k} = \frac{(0.4\text{ Btu/lb-}^0\text{F})}{(110\text{ lb/ft-hr})(1\text{ Btu/ft-lb-}^0\text{F})} = 44.00$$

Coefficients of heat transfer of drilling fluid in drillpipe and annulus are,

$$h_p = 0.023[N_{RE}]^{0.8}[N_{\Pr}]^{0.4}\frac{k}{2r_{pi}} = (0.023)(2746.7)^{0.8}(44)^{0.4}\frac{(12\text{ in/ft})(2)(1\text{ Btu/ft-lb-}^0\text{F})}{(6.375\text{ in})}$$

$$h_p = 110.88\text{ Btu/hr-sq ft-}^o\text{F}$$

$$h_a = 0.023[N_{RE}]^{0.8}[N_{\Pr}]^{0.4}\frac{k}{2r_{wb}} = (0.023)(879.28)^{0.8}(44)^{0.4}\frac{(12\text{ in/ft})(2)(1\text{ Btu/ft-lb-}^0\text{F})}{(9.625\text{ in})}$$

$$h_a = 29.53\text{ Btu/hr-sq ft-}^o\text{F}$$

Overall heat transfer coefficients are calculated by using following equations,

$$\frac{1}{U_p} = \frac{1}{\left(110.88 \text{ Btu/hr-sq ft-}^0\text{F}\right)} + \frac{\left(6.375 \text{ in}\right)}{\left(600\text{Btu/ft-lb-}^0\text{F}\right)\left(2\right)\left(12 \text{ in/ft}\right)} Ln\left(\frac{6.625 \text{ in}}{6.375 \text{ in}}\right)$$
$$+ \frac{\left(6.375 \text{ in}\right)}{\left(6.625 \text{ in}\right)} \frac{1}{\left(29.53 \text{ Btu/hr-sq ft-}^0\text{F}\right)}$$

$$U_p = 24.03 \text{ Btu/hr-sq ft-}^o\text{F}$$

$$\frac{1}{U_a} = \frac{1}{h_a} + \frac{r_{ci3}}{k_{p3}} Ln\left(\frac{r_{co3}}{r_{ci3}}\right) + \frac{r_{ci3}}{k_{e3}} Ln\left(\frac{r_{ci2}}{r_{co3}}\right) + \frac{r_{ci2}}{k_{p2}} Ln\left(\frac{r_{co2}}{r_{ci2}}\right)$$
$$+ \frac{r_{ci2}}{k_{e2}} Ln\left(\frac{r_{ci1}}{r_{co2}}\right) + \frac{r_{ci1}}{k_{p1}} Ln\left(\frac{r_{co1}}{r_{ci1}}\right) + \frac{r_{ci1}}{k_{e1}} Ln\left(\frac{r_{wb}}{r_{ci1}}\right)$$

$$U_a = 16.85 \text{ Btu/hr-sq ft-}^o\text{F}$$

Dimensionless temperature function is,

$$\alpha = \frac{k_f}{c_f \rho_f} = \frac{\left(1.3 \text{ Btu/(ft-}^o\text{F-hr)}\right)}{\left(0.2 \text{ Btu/(lb-}^o\text{F)}\right)\left(165 \text{ lb/ft3}\right)} = 0.039 \text{ sq ft/hr}$$

$$t_D = \frac{\alpha t}{r_{wb}^2} = \frac{\left(0.039 \text{ sq ft/hr}\right)\left(44 \text{ hr}\right)}{\left[\frac{\left(15 \text{ in}\right)}{\left(2\right)\left(12 \text{ in/ft}\right)}\right]^2} = 4.41 \quad > 1.5$$

$$T_D = \left[0.4063 + 0.5 \ln\left(4.41 \quad \right)\right] \times \left(1 + \frac{0.6}{\left(4.41 \quad \right)}\right) = 1.307$$

Derivation constants are,

$$A = \frac{2\pi r_{pi} U_p}{mc_p} = \frac{\pi(2)(6.375\text{ in})(24.03\text{ Btu/hr-sq ft-oF})}{(2)(12\text{ in/ft})(300\text{ B/hr})(10\text{ lb/gal})(42\text{ gal/B})(600\text{Btu/ft-lb-}^0\text{F})}$$

$$A = 0.00080$$

$$B = \frac{2\pi r_{ci} U_a k_f}{mc_p\left(k_f + r_{ci} U_a T_D\right)} = \frac{\pi(2)(9.625\text{ in})(16.85\text{ Btu/hr-sq ft-oF})(1.3\text{ Btu/(ft-}^{\circ}\text{F-hr)})}{(2)(12\text{ in/ft})(300\text{ B/hr})(10\text{ lb/gal})(42\text{ gal/B})(600\text{Btu/ft-lb-}^0\text{F})}$$

$$\frac{1}{\left[(1.3\text{ Btu/(ft-}^{\circ}\text{F-hr)}) + \frac{(9.625\text{ in})}{(2)(12\text{ in/ft})}(16.85\text{ Btu/hr-sq ft-oF})(1.307))\right]}$$

$$B = 0.000108$$

$$\theta_1 = \frac{B + \sqrt{B^2 + 4AB}}{2} = 0.000352$$

$$\theta_2 = \frac{B - \sqrt{B^2 + 4AB}}{2} = -0.000244$$

$$C_1 = \frac{\left(T_{pi} - T_s + \frac{G}{A}\right)\theta_2 e^{\theta_2 H} - G}{\left(\theta_1 e^{\theta_1 H} - \theta_2 e^{\theta_2 H}\right)} = -0.186$$

$$C_2 = \frac{\left(T_{pi} - T_s + \frac{G}{A}\right)\theta_1 e^{\theta_1 H} - G}{\left(\theta_1 e^{\theta_1 H} - \theta_2 e^{\theta_2 H}\right)} = 31.28$$

Applying the final equations to obtain temperature in drillpipe and annulus yields,

$$T_p = C_1 e^{\theta_1 x} + C_2 e^{\theta_2 x} + Gx + T_s - \frac{G}{A}$$

$$T_p = (-0.186)\, e^{(0.000352)(2500\ \text{ft})} + (31.28)\, e^{(-0.000244)(2500\ \text{ft})}$$
$$+ (0.0127\ ^{\circ}\text{F/ft})(2500\ \text{ft}) + (59.5\ ^{\circ}\text{F}) - \frac{(0.0127\ ^{\circ}\text{F/ft})}{(0.00080)}$$

$$T_p = \mathbf{91.83\ ^{o}F}$$

$$T_a = \left(1 + \frac{\theta_1}{A}\right) C_1 e^{\theta_1 x} + \left(1 + \frac{\theta_2}{A}\right) C_2 e^{\theta_2 x} + Gx + T_s$$

$$T_a = \left(1 - \frac{(-0.186)}{(0.00080)}\right) e^{(0.000352)(2500\ \text{ft})} + \left(1 + \frac{(31.28)}{(0.00080)}\right) e^{(-0.000244)(2500\ \text{ft})}$$
$$+ (0.0127\ ^{\circ}\text{F/ft})(2500\ \text{ft}) + (59.5\ ^{\circ}\text{F})$$

$$T_a = \mathbf{102.38\ ^{o}F}$$

APPENDIX D

A Sample Simulation Run

Output of a simulation run made with the 1640 ft well model at 6.85 ^{o}F/100ft geothermal gradient, 500 bbl/hr flow rate, 77 ^{o}F pipe inlet temperature, 59.54 oF surface temperature, thermal properties of formation given in Table 1 and thermal and rehologic properties of the fluid given in Table 1, is presented for 5, 20, 50, 100 and 200 hours of circulation time respectively in Figure 28.

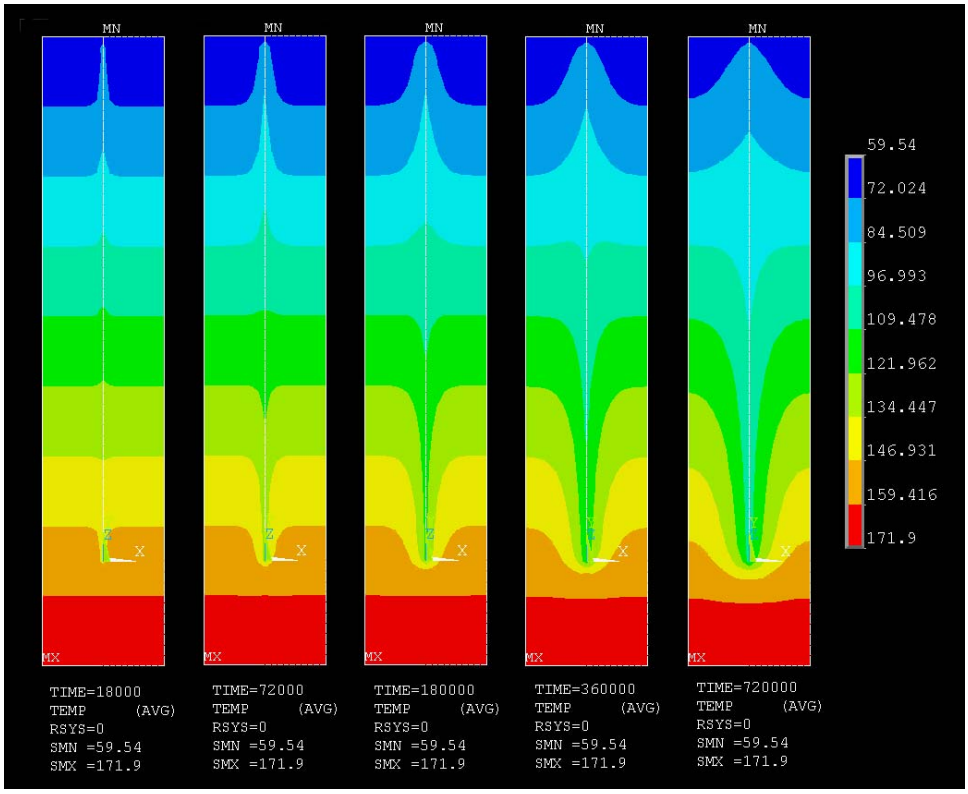

Figure 28. Sample simulation run.